

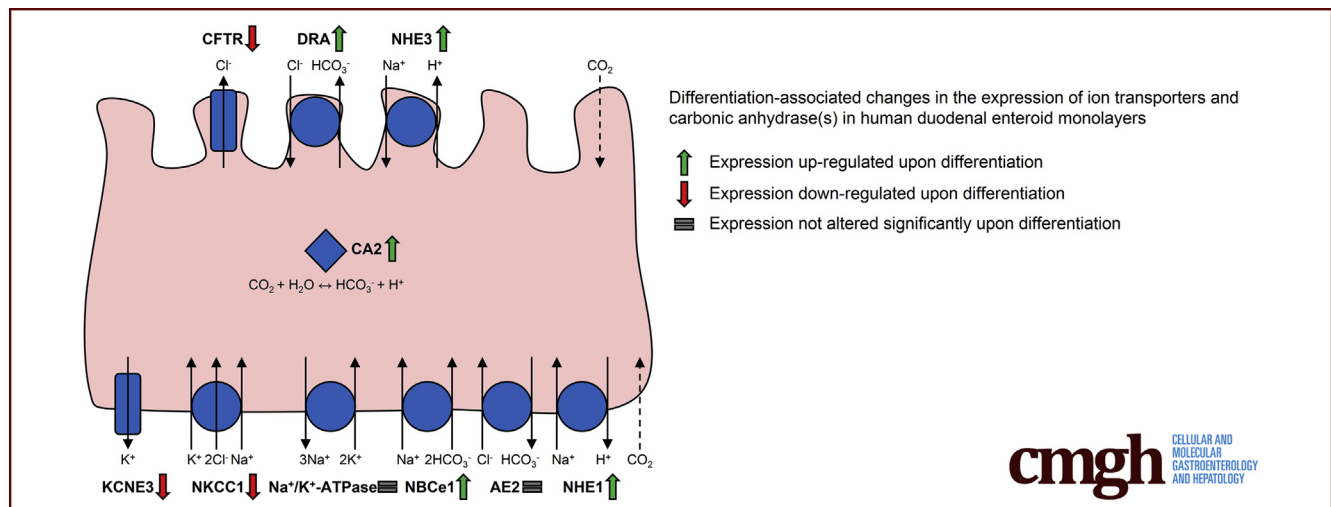
## ORIGINAL RESEARCH

## Molecular Basis and Differentiation-Associated Alterations of Anion Secretion in Human Duodenal Enteroid Monolayers



Jianyi Yin,<sup>1</sup> Chung-Ming Tse,<sup>1</sup> Leela Rani Avula,<sup>1</sup> Varsha Singh,<sup>1</sup> Jennifer Foulke-Abel,<sup>1</sup> Hugo R. de Jonge,<sup>2</sup> and Mark Donowitz<sup>1,3</sup>

<sup>1</sup>Department of Medicine, Division of Gastroenterology and Hepatology, <sup>3</sup>Department of Physiology, Johns Hopkins University School of Medicine, Baltimore, Maryland; <sup>2</sup>Department of Gastroenterology and Hepatology, Erasmus University Medical Center, Rotterdam, The Netherlands



cmgh CELLULAR AND MOLECULAR GASTROENTEROLOGY AND HEPATOLOGY

## SUMMARY

We describe the molecular basis of cyclic adenosine monophosphate-stimulated anion secretion in 2-dimensional human duodenal enteroids and show that active chloride and bicarbonate secretion occur in both crypt-like-undifferentiated and villus-like-differentiated enteroids.

**BACKGROUND & AIMS:** Human enteroids present a novel tool to study human intestinal ion transport physiology and pathophysiology. The present study describes the contributions of Cl<sup>-</sup> and HCO<sub>3</sub><sup>-</sup> secretion to total cyclic adenosine monophosphate (cAMP)-stimulated electrogenic anion secretion in human duodenal enteroid monolayers and the relevant changes after differentiation.

**METHODS:** Human duodenal enteroids derived from 4 donors were grown as monolayers and differentiated by a protocol that includes the removal of Wnt3A, R-spondin1, and SB202190 for 5 days. The messenger RNA level and protein expression of selected ion transporters and carbonic anhydrase isoforms were determined by quantitative real-time polymerase chain reaction and immunoblotting, respectively. Undifferentiated and differentiated enteroid monolayers were mounted in the Ussing chamber/voltage-current clamp apparatus, using solutions that contained as well as lacked

Cl<sup>-</sup> and HCO<sub>3</sub><sup>-</sup>/CO<sub>2</sub>, to determine the magnitude of forskolin-induced short-circuit current change and its sensitivity to specific inhibitors that target selected ion transporters and carbonic anhydrase(s).

**RESULTS:** Differentiation resulted in a significant reduction in the messenger RNA level and protein expression of cystic fibrosis transmembrane conductance regulator, (CFTR) Na<sup>+</sup>/K<sup>+</sup>/2Cl<sup>-</sup> co-transporter 1 (NKCC1), and potassium channel, voltage gated, subfamily E, regulatory subunit 3 (KCNE3); and, conversely, increase of down-regulated-in-adenoma (DRA), electrogenic Na<sup>+</sup>/HCO<sub>3</sub><sup>-</sup> co-transporter 1 (NBCe1), carbonic anhydrase 2 (CA2), and carbonic anhydrase 4 (CA4). Both undifferentiated and differentiated enteroids showed active cAMP-stimulated anion secretion that included both Cl<sup>-</sup> and HCO<sub>3</sub><sup>-</sup> secretion as the magnitude of total active anion secretion was reduced after the removal of extracellular Cl<sup>-</sup> or HCO<sub>3</sub><sup>-</sup>/CO<sub>2</sub>. The magnitude of total anion secretion in differentiated enteroids was approximately 33% of that in undifferentiated enteroids, primarily owing to the reduction in Cl<sup>-</sup> secretion with no significant change in HCO<sub>3</sub><sup>-</sup> secretion. Anion secretion was consistently lower but detectable in differentiated enteroids compared with undifferentiated enteroids in the absence of extracellular Cl<sup>-</sup> or HCO<sub>3</sub><sup>-</sup>/CO<sub>2</sub>. Inhibiting CFTR, NKCC1, carbonic anhydrase(s), cAMP-activated K<sup>+</sup> channel(s), and Na<sup>+</sup>/K<sup>+</sup>-adenosine triphosphatase reduced cAMP-stimulated anion secretion in both undifferentiated and differentiated enteroids.

**CONCLUSIONS:** Human enteroids recapitulate anion secretion physiology of small intestinal epithelium. Enteroid differentiation is associated with significant alterations in the expression of several ion transporters and carbonic anhydrase isoforms, leading to a reduced but preserved anion secretory phenotype owing to markedly reduced  $\text{Cl}^-$  secretion but no significant change in  $\text{HCO}_3^-$  secretion. (*Cell Mol Gastroenterol Hepatol* 2018;5:591–609; <https://doi.org/10.1016/j.jcmgh.2018.02.002>)

**Keywords:** Chloride Secretion; Bicarbonate Secretion; DRA; Ion Transport.

**I**on transport is an essential physiological function of the small intestine. Under physiological conditions, intestinal ion transport is coordinated by intricate regulation of intracellular and extracellular signals.<sup>1</sup> Over the past few decades, our knowledge of intestinal ion transport has been revolutionized owing to the application of molecular biology techniques. To date, the critical transporters mediating the absorption and secretion of major ions have been identified and characterized. Nevertheless, further investigation has been limited in a number of aspects, in large part because of the lack of a reliable and complex model system that faithfully recapitulates human intestinal ion transport physiology and pathophysiology. For instance, many observations in animal models are not reproducible in human subjects,<sup>2</sup> which is also an important reason for the failure of many drug development efforts that begin with great potential in animal studies but turn out to lack clinical effectiveness and safety.<sup>3</sup> In addition, much of our knowledge of intestinal ion transport is based on the findings in nonphysiological cell models such as transfected nonpolarized cells and immortalized cancer cell lines. These results should be interpreted with caution because these models may either show abnormal behavior in particular aspects as a result of genetic instability or fail to present the complex coordination of ion transporters that occurs in the intact human intestine.

To date, the spatial difference in ion transport along the crypt-villus axis of the small intestine remains not fully understood. It is widely believed that absorption and secretion are 2 distinct functions occurring at different sites of the intestinal epithelium, with the former occurring in villi and the latter in crypts. However, a number of studies have suggested that the 2 transport processes may not be completely spatially separated along the crypt-villus axis, and reasons why this separation is unlikely to be so distinct have been described.<sup>1,4–7</sup> In addition, a previous study from our group showed the expression and function of  $\text{Na}^+/\text{H}^+$  exchanger 3 (NHE3), which is responsible for the majority of electro-neutral sodium absorption in the small intestine and a potential drug target for treating diarrhea/constipation,<sup>8</sup> in both crypt-like-undifferentiated enteroids and villus-like-differentiated enteroids, suggesting sodium absorption is not confined to villi.<sup>9</sup> Also, several ion transporters that are thought to contribute to anion secretion, including cystic fibrosis transmembrane conductance regulator (CFTR),  $\text{Na}^+/\text{K}^+/\text{2Cl}^-$  co-transporter 1 (NKCC1), and electrogenic  $\text{Na}^+/\text{HCO}_3^-$  co-transporter 1 (NBCe1), were detectable by

immunofluorescence in rat villus enterocytes and co-localized with NHE3.<sup>5</sup> CFTR, NBCe1, and, to a lesser extent NKCC1, also were documented as being expressed in human villus enterocytes (Turner JR, unpublished data). Moreover, a chloride-dependent depolarization of apical membrane potential difference was observed upon administration of secretagogues in villi as well as in crypts of rat small intestine.<sup>10</sup> Hence, it is reasonable to speculate that anion secretion also may occur in villi, although the extent may not be as large as it is in crypts.<sup>1</sup> However, this speculation lacks strong evidence from human studies, largely owing to the lack of a reliable method to functionally and physically separate crypt cells and villus cells of human small intestinal epithelium.

Recently, primary cultures of adult stem cell-derived intestinal epithelium, called *enteroids*, have presented a novel model for studying intestinal health and disease.<sup>11–14</sup> Our group has reported the use of 3-dimensional human enteroids as a tool to study ion transport processes and has shown a functional similarity between human enteroids and human small intestine in ion transport physiology and pathophysiology.<sup>9,13</sup> We also confirmed the ability to differentiate enteroids by removing specific ingredients from the culture medium that leads to a separation of undifferentiated enteroids, which have crypt-like properties, and differentiated enteroids, which have villus-like properties, respectively.<sup>9,15</sup> This has allowed us to study the spatial difference in cell biology/physiology along the crypt-villus axis of the small intestine. Furthermore, our recent development of 2-dimensional enteroid monolayer cultures has greatly expanded our ability to study enteroids using a variety of approaches, including the Ussing chamber/voltage-current clamp technique for quantitating active electrogenic ion transport processes.<sup>13,15,16</sup>

In this study, we used the model of human duodenal enteroid monolayers to investigate cyclic adenosine monophosphate (cAMP)-stimulated anion secretion. The aim was to determine the molecular basis of anion secretion and the relevant changes upon enteroid differentiation. We herein report that cAMP-stimulated anion secretion in human duodenal enteroids is composed primarily of  $\text{Cl}^-$  secretion with a smaller component of  $\text{HCO}_3^-$  secretion, and is highly dependent on CFTR, NKCC1, cAMP-activated  $\text{K}^+$  channel(s),  $\text{Na}^+/\text{K}^+$ -adenosine triphosphatase (ATPase),

**Abbreviations used in this paper:** AE2, anion exchanger 2; CA, carbonic anhydrase; cAMP, cyclic adenosine monophosphate; CFTR, cystic fibrosis transmembrane conductance regulator;  $\Delta I_{sc}$ , change in short-circuit current; DRA, down-regulated-in-adenoma;  $I_{sc}$ , short-circuit current; KRB, Krebs–Ringer bicarbonate; mRNA, messenger ribonucleic acid; NBC,  $\text{Na}^+/\text{HCO}_3^-$  co-transporter; NBCe1, electrogenic  $\text{Na}^+/\text{HCO}_3^-$  co-transporter 1; NHE,  $\text{Na}^+/\text{H}^+$  exchanger; NKCC1,  $\text{Na}^+/\text{K}^+/\text{2Cl}^-$  co-transporter 1; qRT-PCR, quantitative real-time polymerase chain reaction; SDS, sodium dodecyl sulfate; SITS, 4-Acetamido-4'-isothiocyanato-2,2'-stilbenedisulfonic acid disodium salt hydrate; TER, transepithelial electrical resistance.

 Most current article

© 2018 The Authors. Published by Elsevier Inc. on behalf of the AGA Institute. This is an open access article under the CC BY-NC-ND license (<http://creativecommons.org/licenses/by-nc-nd/4.0/>).

2352-345X

<https://doi.org/10.1016/j.jcmgh.2018.02.002>

and carbonic anhydrase(s). Many of these ion transporters and carbonic anhydrase isoforms are subject to regulation by differentiation at both the messenger RNA (mRNA) and protein levels, contributing to a quantitatively reduced but preserved secretory phenotype of differentiated enteroids.

## Materials and Methods

This study was approved by the Institutional Review Board of Johns Hopkins University School of Medicine (NA\_00038329). All authors had access to the study data and reviewed and approved the final manuscript.

### Propagation of Human Enteroid Cultures

The primary cultures of human enteroids were established using a protocol with minor modifications from the method developed by Sato et al,<sup>11,17</sup> as previously described.<sup>9</sup> In brief, de-identified specimens of normal human small intestine (duodenum/jejunum/ileum) were obtained during endoscopic or surgical procedures, from which crypts containing adult stem cells were isolated to develop enteroids. Enteroids were embedded in Matrigel (Corning, Tewksbury, MA) in 24-well plates (Corning), and maintained in expansion medium composed of base medium of advanced Dulbecco's modified Eagle medium/F12 (Life Technologies, Carlsbad, CA) containing 100 U/mL penicillin/streptomycin (Quality Biological, Gaithersburg, MD), 10 mmol/L HEPES (Life Technologies), and  $1 \times$  GlutaMAX (Life Technologies), with 50% Wnt3A conditioned medium (produced by L-Wnt3A cell line, ATCC CRL-2647), 15% R-spondin1-conditioned medium (produced by HEK293T cell line stably expressing mouse R-spondin1; kindly provided by Dr Calvin Kuo, Stanford University, Stanford, CA), 10% Noggin conditioned medium (produced by HEK293T cell line stably expressing mouse Noggin),<sup>18</sup>  $1 \times$  B27 supplement (Life Technologies), 1 mmol/L N-acetylcysteine (Sigma-Aldrich, St. Louis, MO), 50 ng/mL human epidermal growth factor (Life Technologies), 1  $\mu$ g/mL (Leu-15) gastrin (AnaSpec, Fremont, CA), 500 nmol/L A83-01 (Tocris, Bristol, United Kingdom), 10  $\mu$ mol/L SB202190 (Sigma-Aldrich), and 100  $\mu$ g/mL primocin (InvivoGen, San Diego, CA). Enteroids were cultured in a 5% CO<sub>2</sub> atmosphere at 37°C and passaged every 7–12 days. Expansion medium was supplemented with 10  $\mu$ mol/L Y-27632 (Tocris) and 10  $\mu$ mol/L CHIR99021 (Tocris) during the first 2 days after passaging.

### Enteroid Monolayer Formation and Differentiation

Enteroid monolayers were formed as previously described.<sup>15,16</sup> In short, Transwell inserts (polyester membrane with 0.4- $\mu$ m pores; Corning) were coated with 10  $\mu$ g/cm<sup>2</sup> human collagen IV solution (Sigma-Aldrich) and incubated at 37°C for at least 2 hours. Enteroids were harvested, triturated, and added to the top of Transwell inserts after being resuspended in expansion medium. Each Transwell insert received approximately 50–100 enteroid fragments and was maintained with 100  $\mu$ L expansion medium on top and 600  $\mu$ L expansion medium on bottom. Enteroid monolayers were cultured in a 5% CO<sub>2</sub> atmosphere at 37°C. Expansion medium was supplemented with Y-27632 and CHIR99021 during the first 2 days after

seeding. Formation of enteroid monolayers was monitored by morphologic observation using a Zeiss AXIO inverted microscope (Carl Zeiss, Thornwood, NY) and measurement of transepithelial electrical resistance (TER). Once monolayers became confluent, expansion medium was replaced with differentiation medium that was made by substituting Wnt3A, R-spondin1, and SB202190 in the expansion medium with the base medium. Five days later, paired undifferentiated and differentiated enteroid monolayers were studied.

### Quantitative Real-Time Polymerase Chain Reaction

Total RNA was extracted using the PureLink RNA Mini Kit (Life Technologies) according to the manufacturer's protocol. Complementary DNA was synthesized from 1 to 2  $\mu$ g of RNA using SuperScript VILO Master Mix (Life Technologies). Quantitative real-time polymerase chain reaction (qRT-PCR) was performed using Power SYBR Green Master Mix (Life Technologies) on a QuantStudio 12K Flex real-time PCR system (Applied Biosystems, Foster City, CA). Each sample was run in triplicate, and 5 ng RNA-equivalent complementary DNA was used for each reaction. The sequences of gene-specific primers are listed in Table 1. The relative fold changes in mRNA levels of selected ion transporters and carbonic anhydrase isoforms between differentiated enteroids and undifferentiated enteroids (set as 1) were determined using the  $2^{-\Delta\Delta CT}$  method with human 18S ribosomal RNA simultaneously studied and used as the internal control for normalization.

### Immunoblotting

Cell pellets were collected from enteroid monolayers and solubilized in lysis buffer containing 60 mmol/L HEPES, 150 mmol/L NaCl, 3 mmol/L KCl, 5 mmol/L EDTA trisodium, 3 mmol/L ethylene glycol-bis(2-aminoethylether)-N, N, N', N'-tetraacetic acid (EGTA), 1 mmol/L Na<sub>3</sub>PO<sub>4</sub>, and 1% Triton X-100 and protease inhibitor cocktail (Sigma-Aldrich), followed by homogenization by sonication. After centrifugation at 5000 *g* for 10 minutes, the supernatant was collected as the protein lysate. After protein concentration measurement using the bicinchoninic acid method, protein lysates were mixed with 5 $\times$  sodium dodecyl sulfate (SDS) buffer and denatured at 70°C for 10 minutes. The protocol was slightly modified for the detection of CFTR and down-regulated-in-adenoma (DRA), in which case protein lysates were mixed with 5 $\times$  SDS buffer and incubated at 37°C for 10 minutes. Unless otherwise specified, proteins were separated by SDS-polyacrylamide gel electrophoresis on 4%–20% Mini-Protean TGX Precast Gel (Bio-Rad, Hercules, CA) and transferred onto nitrocellulose membranes (Bio-Rad). After blocking with 5% nonfat milk, blots were probed with primary antibodies overnight at 4°C and IRDye-conjugated secondary antibodies against rabbit and mouse immunoglobulin G (LI-COR, Lincoln, NE) for 1 hour at room temperature. Finally, blots were scanned using an Odyssey CLx imaging system (LI-COR) and the protein bands were visualized and quantified using Image Studio software (LI-COR). The primary antibodies used in this study are listed in Table 2. Glyceraldehyde-3-phosphate dehydrogenase (GAPDH) was used as the loading control.

**Table 1.** Gene-Specific Primers for qRT-PCR

Gene	Forward (5'-3')	Reverse (5'-3')
AE2	TCCCTCTCCTTCCGCAGT	TGCTGGTCCAGATCCAAGA
ATP1A1	ACAGACTTGAGCCGGGGATTA	TCCATTGAGGAGTAGTGGGAG
ATP1B1	CCGGTGGCAGTTGGTTTAAGA	GCATCACTTGGATGGTTCCGA
CA1	TTGAGGACAACGATAACCGATCA	CTACGTGAAGCTCGGCAGAAT
CA2	CACCCCTCCTCTTCTGGAAT	AGTTTACGGAATTTCAACACCTG
CA4	CTGGTGCTACGAGGTTCAAGC	GAAGAAGAAGCGTCCCAGTTT
CA9	CCTTTGCCAGAGTTGACGAG	GCAACTGCTCATAGGCACTG
CFTR	GAAGTAGTGATGGAGAATGTAACAGC	GCTTTCTCAAATAATTCCCCAAA
DRA	CCATCATCGTGCTGATTGTC	AGCTGCCAGGACGGACTT
GATA4	GGAAGCCCAAGAACCTGAAT	GTTGCTGGAGTTGCTGGAA
KCNE3	TTAAGGGAGGTCGCTACTGG	ATGCACAAGGCTTCGGTCTA
KCNQ1	GCTTTTCTAATAAACGTGGAGAA	GGAACCAAGGTGAGAGCAGT
Ki67	GAGGTGTGCAGAAAATCCAAA	CTGTCCCTATGACTTCTGGTTGT
LGR5	ACCAGACTATGCCTTTGGAAAC	TTCCCAGGGAGTGGATTCTAT
NBCe1	CCTCAAGCATGTGTGTGATGA	ACTCTTCGGCACATGGACTC
NBCn1	GCAAGAAACATTCTGACCCTCA	GCTTCCACCCTTCCATTACCT
NHE1	TCTTCACCGTCTTTGTGCAG	ATGGAGCGCTTCGTCTCTT
NHE2	CTTCCACTTCAACCTCCCGAT	GCTGCTATTGCCATCTGCAA
NHE3	GTCTTCCTCAGTGGGCTCAT	ATGAGGCTGCCAAACAGG
NKCC1	AAAGGAACATTCAAGCACAGC	CTAGACACAGCACCTTTTCGTG
PAT-1	TCTACCAGTTCATTGTTCCAGAGGA	GAGAGGGTAGGTCTTCCAAGG
SI	TTTTGGCATCCAGATTCGAC	ATCCAGGCAGCCAAGAATC
18S	GCAATTATTCCTCCATGAACG	GGGACTTAATCAACGCAAGC

ATP1A1, Na<sup>+</sup>/K<sup>+</sup>-adenosine triphosphatase  $\alpha$ -1 subunit; ATP1B1, Na<sup>+</sup>/K<sup>+</sup>-adenosine triphosphatase  $\beta$ -1 subunit; KCNE3, potassium channel, voltage gated, subfamily E, regulatory subunit 3; KCNQ1, potassium channel, voltage gated, subfamily Q, member 1; LGR5, leucine-rich repeat-containing G-protein-coupled receptor 5; NBCn1, electroneutral Na<sup>+</sup>/HCO<sub>3</sub><sup>-</sup> co-transporter 1; PAT-1, putative anion transporter 1.

### Transepithelial Electrical Resistance

TER was measured using an EVOM2 epithelial voltohmmeter (World Precision Instruments, Sarasota, FL) before refreshing the medium. The readings of the voltohmmeter were normalized by the surface area of Transwell inserts (0.33 cm<sup>2</sup>) to calculate the unit area of resistance ( $\Omega$ cm<sup>2</sup>).

### Ussing Chamber/Short-Circuit Current Measurement

Transwell inserts carrying enteroid monolayers were mounted in Ussing chambers (Physiological Instruments, San Diego, CA). The apical and basolateral hemichambers were filled with buffer that was gassed continuously with 95% O<sub>2</sub>/5% CO<sub>2</sub>, maintained at 37°C, and connected

**Table 2.** Primary Antibodies for Immunoblotting

Antigen	Manufacturer	Catalog number	Host	Dilution
ATP1A1	Developmental Studies Hybridoma Bank (Iowa City, IA)	a5	Mouse	1:1000
CA2	Novus (Littleton, CO)	NB600-919	Rabbit	1:500
CFTR	Cystic Fibrosis Foundation Therapeutics (Chapel Hill, NC)	217	Mouse	1:400
DRA	Santa Cruz	sc-376187	Mouse	1:200
GAPDH	Sigma-Aldrich	G8795	Mouse	1:5000
NBCe1	Abcam (Cambridge, MA)	ab30322	Rabbit	1:500
NHE2	Provided by Dr Chung-Ming Tse (Johns Hopkins University, Baltimore, MD)	N/A	Rabbit	1:500
NHE3	Novus (Littleton, CO)	NBP1-82574	Rabbit	1:500
NKCC1	Developmental Studies Hybridoma Bank (Iowa City, IA)	T4-C	Mouse	1:1000

ATP1A1, Na<sup>+</sup>/K<sup>+</sup>-adenosine triphosphatase  $\alpha$ -1 subunit; GAPDH, glyceraldehyde-3-phosphate dehydrogenase; N/A, not applicable.

**Table 3.** Compounds for Ussing Chamber/Short-Circuit Current Measurement

Compound	Manufacturer	Final concentration	Side
Acetazolamide	Sigma-Aldrich	250 $\mu\text{mol/L}$	AP + BL
Bumetanide	Sigma-Aldrich	100 $\mu\text{mol/L}$	BL
CFTRinh-172	EMD Millipore (Burlington, MA)	5 or 25 $\mu\text{mol/L}$	AP
Chromanol 293B	Sigma-Aldrich	10 $\mu\text{mol/L}$	BL
Forskolin	Sigma-Aldrich	10 $\mu\text{mol/L}$	BL
Ouabain	Sigma-Aldrich	100 $\mu\text{mol/L}$	BL
S0859	Sigma-Aldrich	30 $\mu\text{mol/L}$	BL
SITS	Sigma-Aldrich	1 mmol/L	BL
Tenapanor	Ardelyx (Fremont, CA)	0.1–1 $\mu\text{mol/L}$	AP

AP, apical; BL, basolateral.

to a voltage-current clamp apparatus (Physiological Instruments) via Ag/AgCl electrodes and 3 mol/L KCl agar bridges. Krebs–Ringer bicarbonate buffer (KRB buffer) consisted of 115 mmol/L NaCl, 25 mmol/L NaHCO<sub>3</sub>, 0.4 mmol/L KH<sub>2</sub>PO<sub>4</sub>, 2.4 mmol/L K<sub>2</sub>HPO<sub>4</sub>, 1.2 mmol/L CaCl<sub>2</sub>, 1.2 mmol/L MgCl<sub>2</sub>, pH 7.4.<sup>19</sup> In Cl<sup>-</sup>-free buffer and HCO<sub>3</sub><sup>-</sup>-free buffer, Cl<sup>-</sup> and HCO<sub>3</sub><sup>-</sup> in KRB buffer were replaced with gluconate. Cl<sup>-</sup>-free buffer was supplemented with an additional 5 mmol/L calcium gluconate to maintain the level of free calcium. HCO<sub>3</sub><sup>-</sup>-free buffer was gassed with 100% O<sub>2</sub> and supplemented with 5 mmol/L HEPES and 1 mmol/L acetazolamide to inhibit the endogenous production of HCO<sub>3</sub><sup>-</sup>/CO<sub>2</sub>. In addition, buffer in the basolateral hemichamber was supplemented with 10 mmol/L glucose as an energy substrate; buffer in the apical hemichamber was supplemented with 10 mmol/L mannitol to maintain the osmotic balance. Current clamping was used, and short-circuit current (I<sub>sc</sub>) and TER were recorded every 20 seconds by Acquire and Analyze software (Physiological Instruments). To investigate the change of short-circuit current ( $\Delta I_{sc}$ ) in response to an apical-basolateral gradient of glucose, 40 mmol/L glucose was added to the apical hemichamber with 40 mmol/L mannitol to the basolateral hemichamber. To investigate cAMP-stimulated anion secretion, 10  $\mu\text{mol/L}$  forskolin was added to the basolateral hemichamber, after which the effects of inhibitors targeting selected ion transporters and carbonic anhydrase(s) were studied (Table 3). The time-course changes in I<sub>sc</sub> and TER were delineated.

### Statistical Analysis

Data are presented as means  $\pm$  SEM. Statistical analyses were conducted using the Student's *t* test with  $P < .05$  considered statistically significant. Studies were performed using 4 duodenal enteroid lines derived from 4 separate normal human subjects unless otherwise specified. In most cases, experiments were repeated multiple times using multiple enteroid lines and the results were analyzed together using a paired *t* test with statistical analysis considering the total number of experiments with paired undifferentiated/differentiated enteroids as the sample size.

In several cases, experimental variability within single enteroid lines was calculated as means  $\pm$  SEM.

## Results

### Phenotypic Changes After Differentiation

In previous studies,<sup>9,15</sup> we reported a 5-day differentiation protocol of human enteroids that allowed the transition of undifferentiated enteroids consisting of stem cells, Paneth cells, and transit-amplifying cells into differentiated enteroids made up primarily of enterocytes, goblet cells, and enteroendocrine cells. In the present study, we further characterized the phenotypic changes in 2-dimensional human duodenal enteroids after 5 days of differentiation. First, there was an increase in TER upon differentiation (Figure 1A and B); 5-day differentiated enteroid monolayers had significantly higher TER than undifferentiated enteroid monolayers (1167  $\pm$  140  $\Omega\text{cm}^2$  vs 371  $\pm$  29  $\Omega\text{cm}^2$ ;  $P < .001$ ), but prolonged differentiation up to 7 days did not cause an additional increase in TER. This is in accordance with our previous observation in human jejunal enteroid monolayers.<sup>15</sup> Second, differentiated enteroid monolayers showed a higher response rate to an apical-basolateral gradient of glucose than undifferentiated enteroid monolayers in the magnitude of maximal increase in I<sub>sc</sub> (15.6  $\pm$  2.9  $\mu\text{A/cm}^2$  vs 7.8  $\pm$  1.5  $\mu\text{A/cm}^2$ ;  $P < .001$ ) (Figure 1C and D), indicating an increase in the apical Na<sup>+</sup>-glucose co-transport activity after differentiation. Third, Sucrase-isomaltase (*SI*), a brush-border glucosidase enzyme and intestinal differentiation marker, was up-regulated significantly at the mRNA level upon differentiation (Figure 1E). Fourth, the mRNA levels of leucine-rich repeat-containing G-protein-coupled receptor 5 (*LGR5*), an intestinal stem cell marker, and *Ki67*, a cellular proliferation marker, were dramatically reduced with differentiation (Figure 1F and G).

In addition, studies were performed to characterize the segment-specific identity of duodenal enteroid monolayers before and after differentiation. GATA4 is an intestinal segment-specific transcription factor that controls the cephalocaudal expression pattern of small intestine by repressing the expression of ileum-specific genes in upper small intestinal segments.<sup>20,21</sup> The current study found that GATA4 mRNA was confined to human enteroid monolayers derived from duodenum and jejunum, and its amount was maintained in duodenum and slightly increased in jejunum after differentiation (Figure 1H). Taken together, these results present additional evidence that the 5-day differentiation protocol allows the separation of crypt-like cells (undifferentiated enteroids) and villus-like cells (differentiated enteroids) without affecting their segment-specific identity in 2-dimensional human duodenal enteroids, encouraging the subsequent investigations on the differentiation-associated modulations of ion transport.

### Expression of Ion Transporters and Carbonic Anhydrase Isoforms Upon Differentiation

To investigate the alterations of ion transport after differentiation, mRNA levels of selected ion transporters and carbonic anhydrase isoforms were examined in

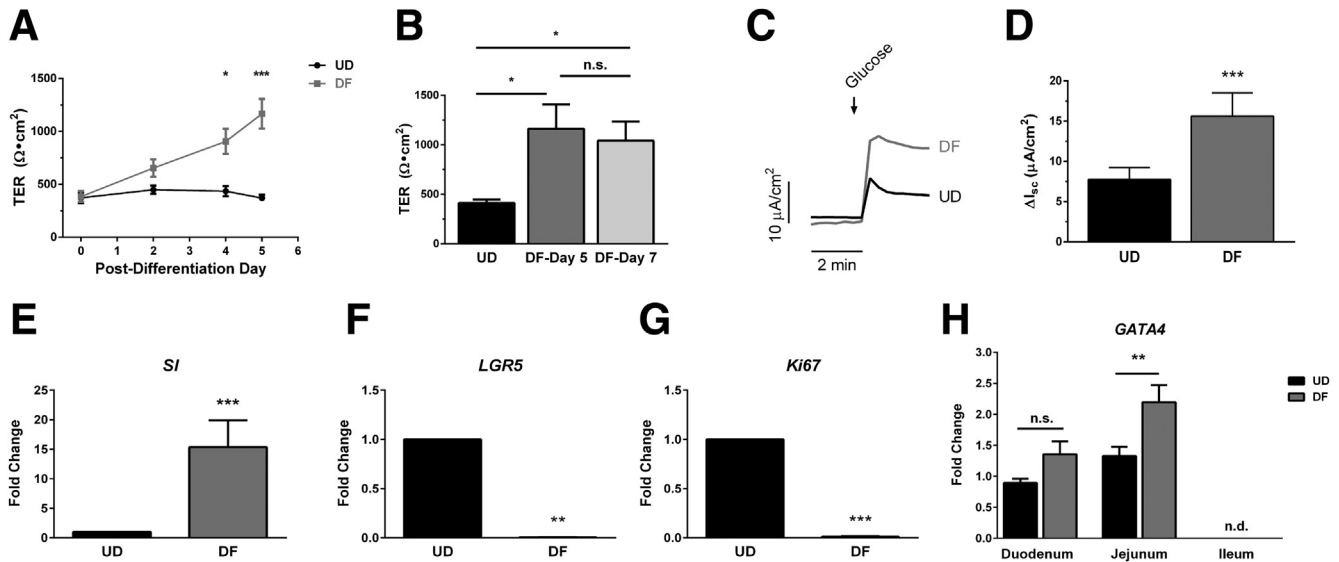


**Figure 1. Phenotypic changes of human enteroid monolayers upon differentiation.** (A) TER of undifferentiated (UD) and differentiated (DF) duodenal enteroid monolayers over time. Differentiated enteroids had a significantly higher TER than undifferentiated enteroids on day 4 ( $*P < .05$ ) and day 5 ( $***P < .001$ ).  $n = 6$  experiments with paired enteroid monolayers derived from 3 donors. (B) There was no difference in TER between duodenal enteroid monolayers that were differentiated for 5 days or 7 days ( $1162 \pm 246 \Omega \cdot \text{cm}^2$  vs  $1042 \pm 193 \Omega \cdot \text{cm}^2$ ,  $P = .06$ ).  $*P < .05$ .  $n = 3$  experiments with paired enteroid monolayers derived from 3 donors. (C and D) A representative trace and quantitative analysis showing a higher response in  $\Delta I_{sc}$  to an apical-basolateral gradient of glucose (30 mmol/L) in differentiated enteroids than undifferentiated enteroids ( $***P < .001$ ).  $n = 4$  experiments with paired enteroid monolayers derived from 4 donors. (E–G) qRT-PCR data showing the mRNA level of sucrase-isomaltase (*SI*) was increased by  $15.4 \pm 4.6$  times upon differentiation, whereas that of leucine-rich, repeat-containing, G-protein-coupled receptor 5 (*LGR5*) and *Ki67* was reduced by  $379 \pm 209$  and  $102 \pm 27$  times, respectively.  $**P < .01$ ,  $***P < .001$ .  $n = 4$ –8 experiments with paired enteroid monolayers derived from 4 donors. (H) qRT-PCR data showing that *GATA4* gene expression was confined to duodenal and jejunal enteroid monolayers with no change in duodenum and a slight increase in jejunum after differentiation.  $**P < .01$ . n.d., not detected (threshold [Ct] value  $>34$ ).  $n = 3$  experiments with paired enteroid monolayers derived from 3 donors (duodenum, jejunum) or 2 donors (ileum).

undifferentiated and differentiated duodenal enteroid monolayers by qRT-PCR. The ion transporters and carbonic anhydrase isoforms selected are known to play important roles in  $\text{Cl}^-$  and  $\text{HCO}_3^-$  secretion, electroneutral  $\text{Na}^+$  absorption, and intracellular pH regulation under physiological and pathophysiological conditions. As shown in Figure 2A, several ion transporters and carbonic anhydrase isoforms were up-regulated significantly at the mRNA level upon differentiation. These included carbonic anhydrase (*CA*)4 (64.4-fold), *DRA* (21.6-fold), *CA2* (4.0-fold), *NHE1* (2.7-fold), *NBCe1* (2.4-fold), and  $\text{Na}^+/\text{K}^+$ -adenosine triphosphatase  $\beta$ -1 subunit (*ATP1B1*) (1.7-fold). In contrast, several ion transporters were down-regulated significantly after differentiation, including *NKCC1* (7.1-fold), potassium channel, voltage gated, subfamily E, regulatory subunit 3 (*KCNE3*) (5.2-fold), and *CFTR* (2.7-fold). The mRNA levels of the following ion transporters and carbonic anhydrase isoforms were not significantly changed by differentiation: anion exchanger 2 (*AE2*),  $\text{Na}^+/\text{K}^+$ -adenosine triphosphatase  $\alpha$ -1 subunit (*ATP1A1*), *CA1*, *CA9*, potassium channel, voltage gated, subfamily Q, member 1 (*KCNQ1*), electroneutral  $\text{Na}^+/\text{HCO}_3^-$  cotransporter 1 (*NBCe1*), *NHE2*, *NHE3*, and putative anion transporter 1 (*PAT-1*). The qRT-PCR threshold values are shown in Figure 2B. Most of these findings in 2-dimensional enteroids were consistent with the results obtained from in parallel studies of 3-dimensional enteroids (Figure 3).

We further studied the protein expression of selected ion transporters and carbonic anhydrase isoforms in undifferentiated and differentiated duodenal enteroid monolayers by immunoblotting (Figure 4A and B). Consistent with the results of qRT-PCR, *CFTR* (2.0-fold) and *NKCC1* (4.0-fold) were down-regulated significantly at the protein level, *CA2* (2.5-fold), *DRA* (4.6-fold) and *NBCe1* (2.3-fold) were up-regulated significantly, and *ATP1A1* and *NHE2* were not changed upon differentiation. Although there was no significant change at the mRNA level, the protein expression of *NHE3* was slightly but significantly up-regulated by 1.5-fold after differentiation. In sum, these data suggest a significant regulatory effect of differentiation on the expression of multiple ion transporters and carbonic anhydrase isoforms, some of which are known to be essential for intestinal  $\text{Cl}^-$  and  $\text{HCO}_3^-$  secretion.

### Reduced cAMP-Stimulated Anion Secretion Upon Differentiation

To study anion secretion at the functional level, Transwell inserts carrying paired undifferentiated and differentiated enteroid monolayers were mounted in Ussing chambers, and forskolin was used to induce cAMP-stimulated electrogenic anion secretion as indicated by the increase in short-circuit current. As shown in Figure 5A and D,

in KRB buffer in which extracellular  $\text{Cl}^-$  and  $\text{HCO}_3^-/\text{CO}_2$  are both present, forskolin caused an immediate increase in  $I_{sc}$  in both undifferentiated enteroids ( $34.8 \pm 4.6 \mu\text{A}/\text{cm}^2$ ) and differentiated enteroids ( $10.4 \pm 1.3 \mu\text{A}/\text{cm}^2$ ). Based on the existing knowledge of cAMP/protein kinase A-induced anion secretion, we speculated that cAMP-stimulated anion secretion in KRB buffer consisted of 2 major components, namely  $\text{Cl}^-$  secretion and  $\text{HCO}_3^-$  secretion, and that each component was largely dependent on the presence of extracellular  $\text{Cl}^-$  and  $\text{HCO}_3^-/\text{CO}_2$ , respectively. As such, we investigated whether the removal of extracellular  $\text{Cl}^-$  or  $\text{HCO}_3^-/\text{CO}_2$  reduced cAMP-stimulated secretion. Figure 5B and C show that duodenal enteroid monolayers had a smaller response to forskolin in  $\text{HCO}_3^-$ -free buffer and  $\text{Cl}^-$ -free buffer. Quantitatively, the magnitude of forskolin-induced  $\Delta I_{sc}$  was  $27.7 \pm 4.8 \mu\text{A}/\text{cm}^2$  in  $\text{HCO}_3^-$ -free buffer and  $3.3 \pm 0.6 \mu\text{A}/\text{cm}^2$  in  $\text{Cl}^-$ -free buffer for undifferentiated enteroids, and was  $3.9 \pm 0.9 \mu\text{A}/\text{cm}^2$  in  $\text{HCO}_3^-$ -free buffer and  $0.5 \pm 0.1 \mu\text{A}/\text{cm}^2$  in  $\text{Cl}^-$ -free buffer for differentiated enteroids (Figure 5D). Figure 5E shows the experimental variability by showing the means  $\pm$  SEM of the maximal forskolin response of 4 separate enteroid lines in KRB,  $\text{HCO}_3^-$ -free, and  $\text{Cl}^-$ -free buffer. We further normalized the magnitude of forskolin-induced  $\Delta I_{sc}$  in  $\text{HCO}_3^-$ -free and  $\text{Cl}^-$ -free buffer to that in KRB buffer (set as 100%). As shown in Figure 5F, there was a reduction to  $80\% \pm 7\%$  in  $\text{HCO}_3^-$ -free buffer and  $9\% \pm 2\%$  in  $\text{Cl}^-$ -free buffer for undifferentiated enteroids, and  $41\% \pm 8\%$  in  $\text{HCO}_3^-$ -free buffer and  $5\% \pm 2\%$  in  $\text{Cl}^-$ -free buffer for differentiated enteroids (these data were calculated by considering all experiments within a single enteroid line as  $n = 1$  and are shown as the means  $\pm$  SEM of 4 enteroid lines). These results support the speculation that when extracellular  $\text{Cl}^-$  and  $\text{HCO}_3^-/\text{CO}_2$  are both available, the cAMP-stimulated anion secretion from enteroid monolayers comprises both  $\text{Cl}^-$  and  $\text{HCO}_3^-$  secretion. Furthermore, these results indicate a higher dependency of cAMP-stimulated anion secretion on extracellular  $\text{Cl}^-$  than on extracellular  $\text{HCO}_3^-/\text{CO}_2$ .

We also compared undifferentiated and differentiated enteroids in their response to forskolin in multiple buffers. In KRB buffer, the maximal increase of  $I_{sc}$  in response to forskolin was significantly lower in differentiated enteroids, which was  $33\% \pm 4\%$  of that of undifferentiated enteroids ( $P < .001$ ) (Figure 5G). This is in contrast to our previous finding in 3-dimensional duodenal enteroids that forskolin-induced swelling was greater in differentiated than undifferentiated enteroids.<sup>9</sup> Notably, we have changed the nature of expansion medium for enteroids since the initial report<sup>9</sup> and used the modified expansion medium which lacks nicotinamide in the current study (see the Materials and Methods section).<sup>22</sup> As shown in Figure 5J, when studies were repeated using the modified expansion medium, forskolin-induced swelling was greater in undifferentiated than differentiated 3-dimensional duodenal enteroids. In the present study, the magnitude of forskolin-induced  $\Delta I_{sc}$  in duodenal enteroid monolayers was consistently lower in differentiated enteroids compared with undifferentiated enteroids in multiple buffer conditions:  $16\% \pm 3\%$  of that of

undifferentiated enteroids in  $\text{HCO}_3^-$ -free buffer ( $P < .001$ ) (Figure 5H) and  $15\% \pm 2\%$  in  $\text{Cl}^-$ -free buffer ( $P < .001$ ) (Figure 5I). These results show reduced anion secretion after differentiation; however, forskolin-induced  $\Delta I_{sc}$  was still detectable in differentiated enteroids in all buffer conditions, suggesting a preserved anion secretory phenotype in differentiated enteroids.

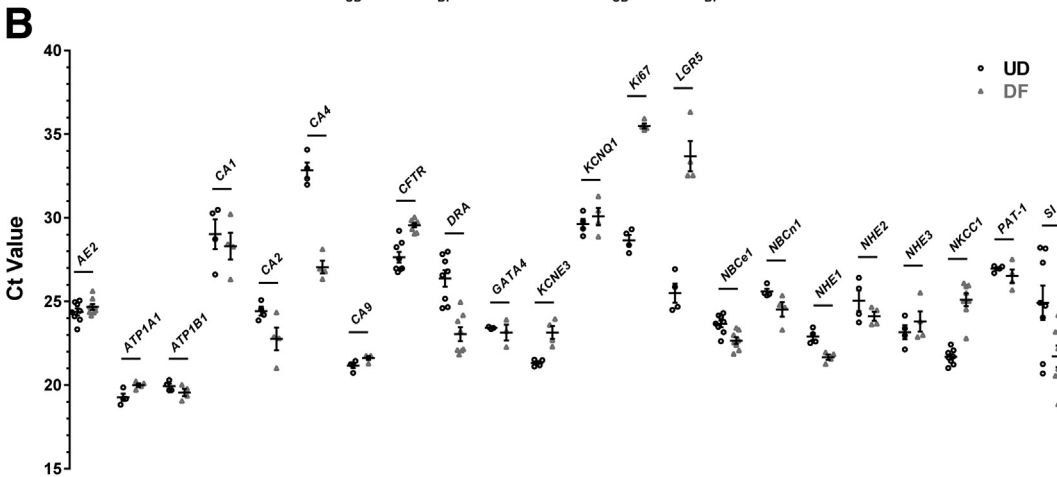
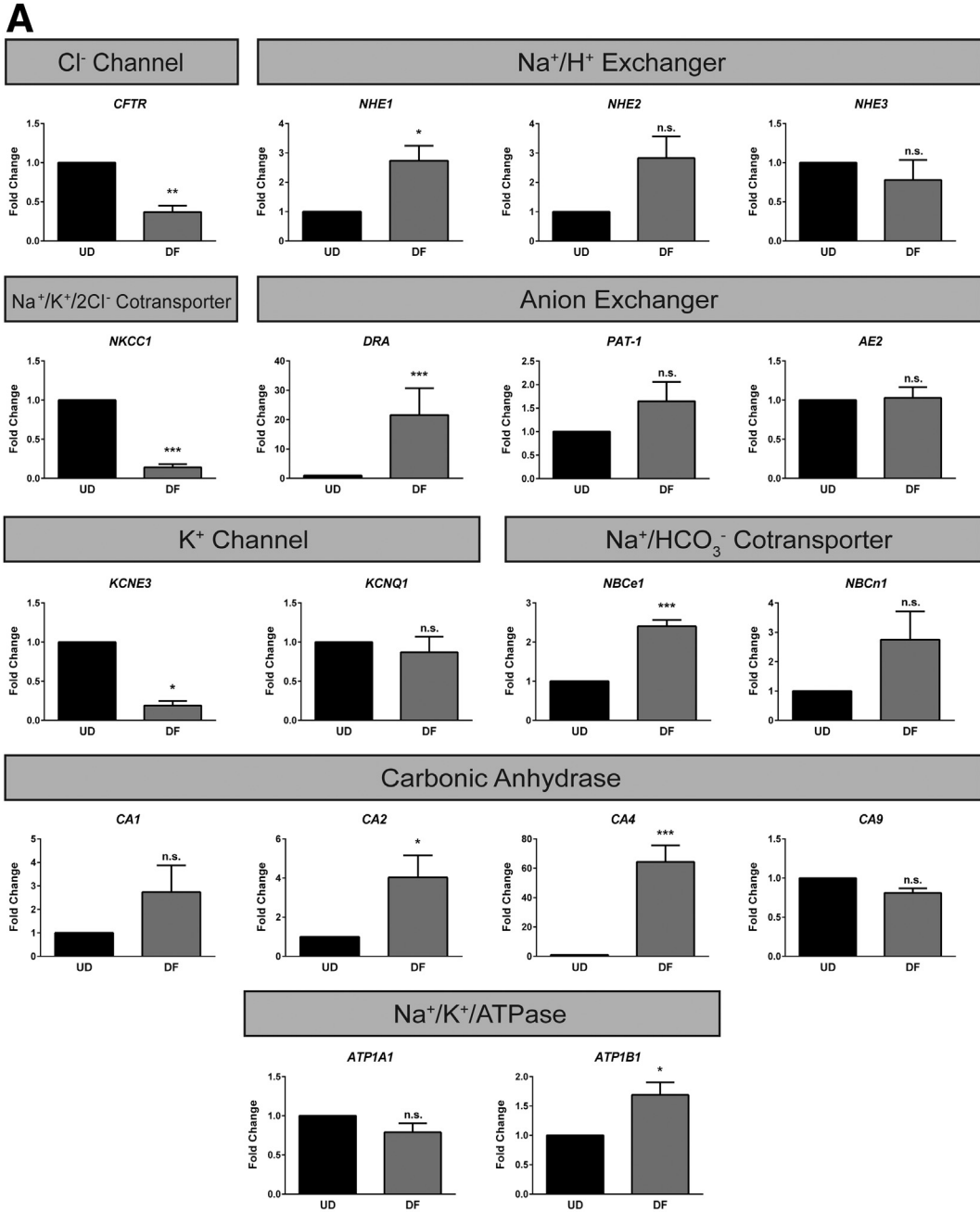
### Apical Ion Transporters in cAMP-Stimulated Anion Secretion

Anion secretion involves multiple ion transporters that are located on the apical and basolateral membranes of intestinal epithelial cells. The contribution of selected ion transporters to cAMP-stimulated anion secretion was determined using specific inhibitors, and the effects of these inhibitors on TER were studied simultaneously (Figure 6). CFTR is an apical ion channel that is permeable to both  $\text{Cl}^-$  and, to a lesser extent,  $\text{HCO}_3^-$ .<sup>23</sup> A previous study showed that blocking CFTR resulted in substantial inhibition of forskolin-induced  $\Delta I_{sc}$  as well as luminal fluid accumulation in jejunal enteroids.<sup>24</sup> In this study, we further confirmed the role of CFTR in cAMP-stimulated anion secretion of duodenal enteroid monolayers using CFTR<sub>inh</sub>-172 as a CFTR blocker. In KRB buffer, CFTR<sub>inh</sub>-172 ( $25 \mu\text{mol}/\text{L}$ ) inhibited  $85\% \pm 3\%$  and  $95\% \pm 8\%$  of forskolin-induced  $\Delta I_{sc}$  in undifferentiated and differentiated enteroids, respectively (Figure 7A and D). A lower dose of CFTR<sub>inh</sub>-172 ( $5 \mu\text{mol}/\text{L}$ ) also inhibited the majority of forskolin-induced  $\Delta I_{sc}$  in KRB buffer ( $84\% \pm 6\%$  for undifferentiated enteroids and  $87\% \pm 6\%$  for differentiated enteroids) (Figure 7E). Similarly, the inhibitory effect of CFTR<sub>inh</sub>-172 ( $25 \mu\text{mol}/\text{L}$ ) of  $90\%$ – $119\%$  of the forskolin-induced  $\Delta I_{sc}$  was observed in  $\text{HCO}_3^-$ -free buffer and  $\text{Cl}^-$ -free buffer (Figure 7B–D).

A previous study by our group reported a potential role of NHE3 in forskolin-induced swelling in 3-dimensional duodenal enteroids, but it was not clear whether NHE3 participates in this process through its role in  $\text{Na}^+$  absorption, anion secretion, or both.<sup>9</sup> To address this, we studied the effect of tenapanor, a novel NHE3 inhibitor with a median inhibitory concentration in the nanomolar range,<sup>8</sup> on forskolin-induced  $\Delta I_{sc}$  in duodenal enteroid monolayers. As shown in Figure 7F, the addition of up to  $1 \mu\text{mol}/\text{L}$  tenapanor did not have any significant effect on forskolin-induced  $\Delta I_{sc}$  in either undifferentiated or differentiated enteroids in KRB buffer. Therefore, NHE3 does not appear to contribute to cAMP-stimulated anion secretion in duodenal enteroids.

### Basolateral Ion Transporters and Carbonic Anhydrase(s) in cAMP-Stimulated Anion Secretion

A number of compounds that target selected basolateral ion transporters and carbonic anhydrase(s) were used to determine their roles in cAMP-stimulated anion secretion. In KRB buffer, administration of bumetanide, a specific blocker of NKCC1, caused a dramatic reduction in forskolin-induced  $\Delta I_{sc}$  in undifferentiated enteroids and a lesser reduction in



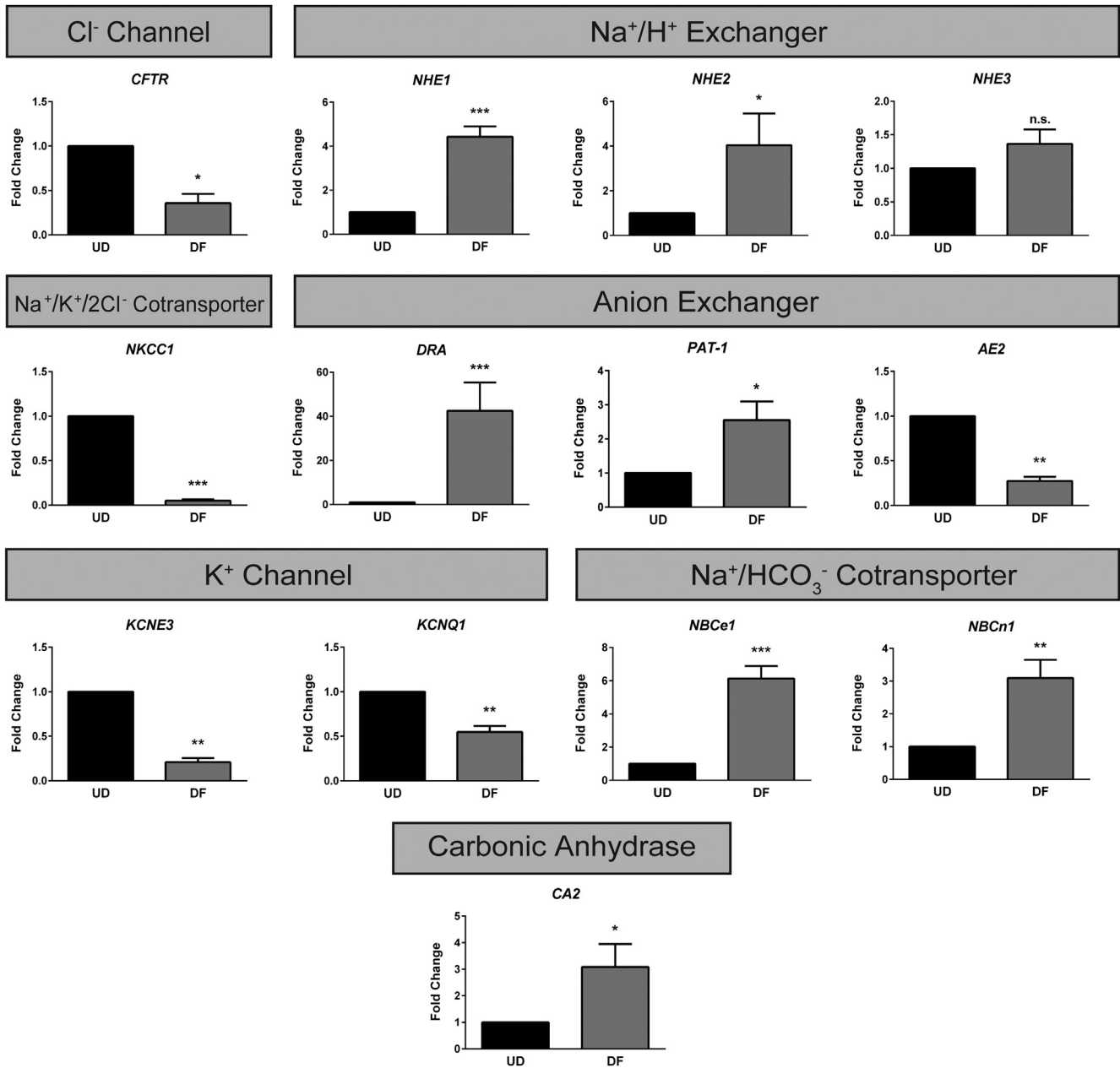


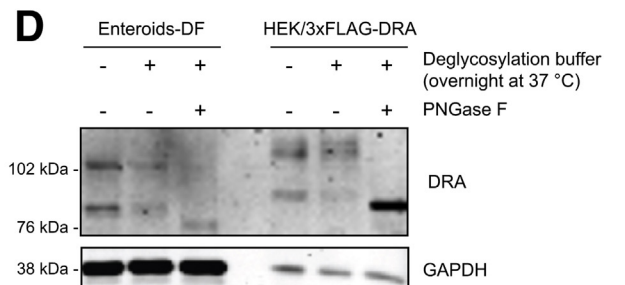
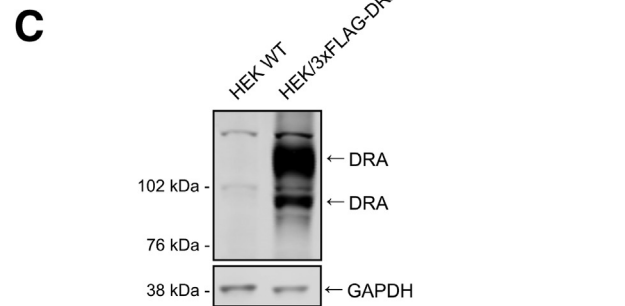
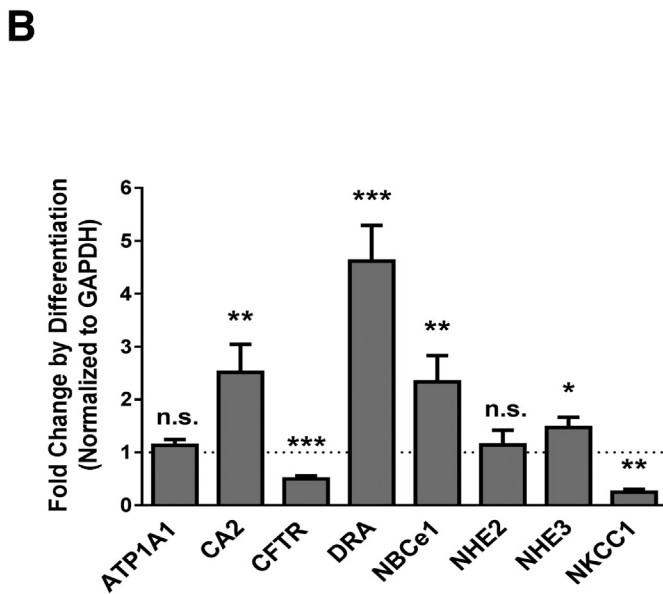
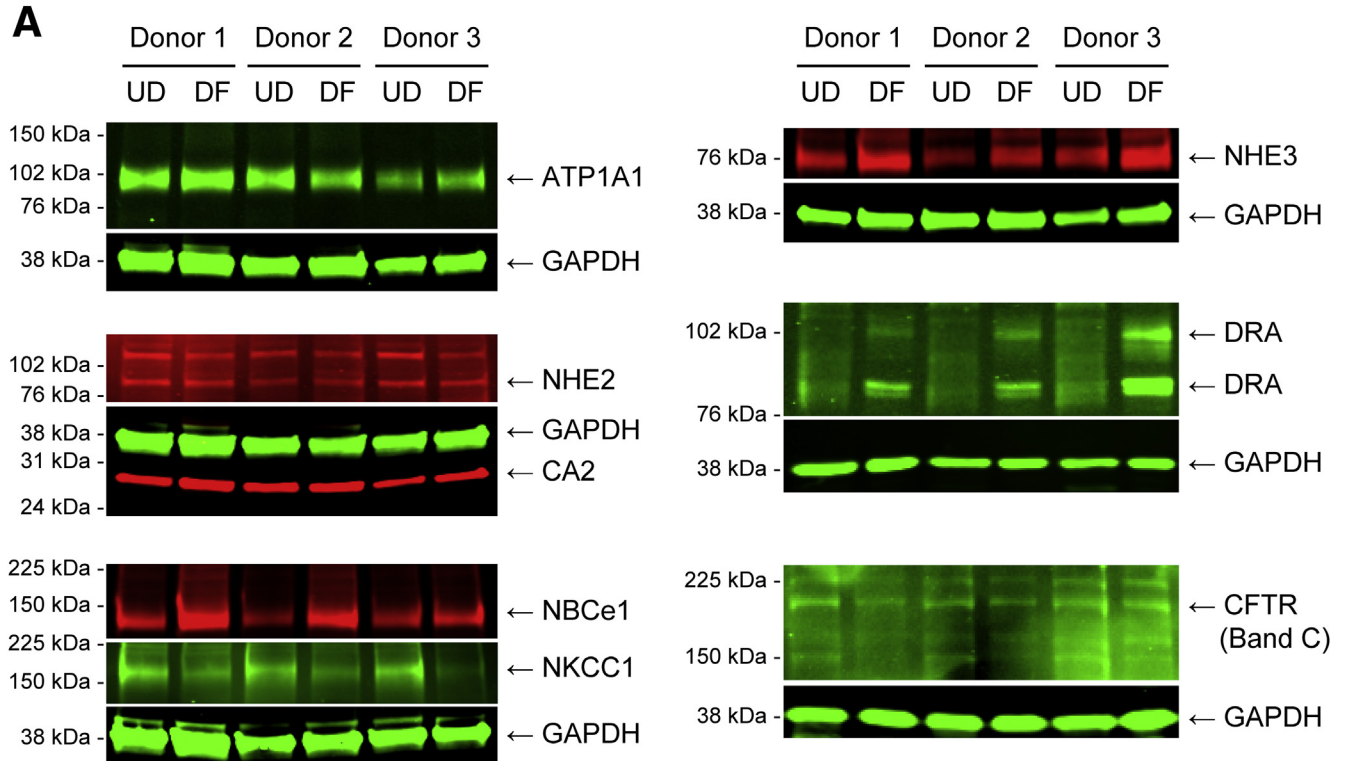
**Figure 3. mRNA level of selected ion transporters and carbonic anhydrase isoforms in 3-dimensional human duodenal enteroids.** The mRNA levels of selected ion transporters and carbonic anhydrase isoforms were determined by qRT-PCR and the relative fold changes between differentiated (DF) and undifferentiated (UD) 3-dimensional enteroids (set as 1) were calculated using 18S ribosomal RNA as the endogenous control. These data are mostly consistent with those of parallel studies in duodenal enteroid monolayers (See results in Figure 2). \**P* < .05, \*\**P* < .01, \*\*\**P* < .001. n = 5 experiments with paired 3-dimensional enteroids derived from 5 donors.

**Figure 2. (See previous page). mRNA levels of selected ion transporters and carbonic anhydrase isoforms in human duodenal enteroid monolayers.** (A) The mRNA levels of selected ion transporters and carbonic anhydrase isoforms were determined by qRT-PCR and the relative fold changes between differentiated (DF) and undifferentiated (UD) enteroid monolayers (set as 1) were calculated using 18S ribosomal RNA as the endogenous control. Most of the results are consistent with those in parallel studies of 3-dimensional duodenal enteroids (See results in Figure 3). \**P* < .05, \*\**P* < .01, \*\*\**P* < .001. n = 4–8 experiments with paired enteroid monolayers derived from 4 donors. (B) Scatter plots showing the threshold [Ct] values of selected genes in undifferentiated and differentiated duodenal enteroid monolayers. Each plot represents the result of a single experiment. A total of 5 ng RNA-equivalent complementary DNA was used for each qRT-PCR reaction. These Ct values were further normalized to 18S ribosomal RNA (Ct value ~ 7–8) to determine the relative amount of each gene in each sample. n = 4–8 experiments with paired enteroid monolayers derived from 4 donors.

differentiated enteroids (Figure 8A). In most cases, a bumetanide-insensitive component was observed, particularly in differentiated enteroids. We then studied whether this bumetanide-insensitive component could be inhibited by acetazolamide, a general carbonic anhydrase inhibitor. As shown in Figure 8A and B, the bumetanide-insensitive component was sensitive to acetazolamide, and the combination of bumetanide and acetazolamide abolished forskolin-induced  $\Delta I_{sc}$  regardless of their order of addition. These results confirm that forskolin-induced  $\Delta I_{sc}$  in KRB

buffer is contributed by  $Cl^-$  secretion and  $HCO_3^-$  secretion as 2 major components, and suggest the involvement of NKCC1 and carbonic anhydrase(s) in cAMP-stimulated anion secretion through their roles in  $Cl^-$  secretion and  $HCO_3^-$  secretion, respectively.

We further compared undifferentiated and differentiated enteroids in their sensitivity to bumetanide and acetazolamide (Figure 8C and D). The bumetanide-sensitive component accounted for a relatively greater percentage in undifferentiated enteroids than differentiated



enteroids ( $75\% \pm 3\%$  vs  $44\% \pm 5\%$ ;  $P < .001$ ), whereas the acetazolamide-sensitive component contributed to a relatively larger percentage in differentiated enteroids than undifferentiated enteroids ( $51\% \pm 8\%$  vs  $13\% \pm 2\%$ ;  $P < .001$ ). We also calculated the absolute reduction in forskolin-induced  $\Delta I_{sc}$  after the addition of acetazolamide (Figure 8E). This represents the acetazolamide-sensitive anion secretion and was very similar between undifferentiated enteroids and differentiated enteroids ( $4.4 \pm 0.8 \mu A/cm^2$  vs  $5.3 \pm 0.9 \mu A/cm^2$ ,  $P = .35$ ).

In addition, we found that cAMP-stimulated anion secretion in duodenal enteroid monolayers required active  $Na^+/K^+$ -ATPase because ouabain caused a decrease in forskolin-induced  $\Delta I_{sc}$  with a rapid onset within 2 minutes of addition (Figure 8F). Moreover, although several previous publications have suggested a potential role of basolateral anion exchangers such as AE2 and sodium/bicarbonate co-transporters such as NBCe1 in anion secretion, the present study failed to validate the functional involvement of these transporters in cAMP-stimulated anion secretion in human duodenal enteroids because there was no evident inhibition of forskolin-induced  $\Delta I_{sc}$  after the administration of disodium 4-acetamido-4'-isothiocyanato-stilben-2,2'-disulfonate (SITS), which inhibits AE2, or S0859, which inhibits the NBC family (Figure 8G and H).<sup>25,26</sup>

### Basolateral Ion Transporters in cAMP-Stimulated $Cl^-$ Secretion

We also studied the functional involvement of several basolateral ion transporters in  $HCO_3^-$ -free buffer, in which forskolin-induced  $\Delta I_{sc}$  was completely attributed to electrogenic  $Cl^-$  secretion via CFTR. In the absence of  $HCO_3^-/CO_2$ , inhibition of NKCC1 by bumetanide abolished forskolin-induced  $\Delta I_{sc}$  in both undifferentiated enteroids ( $97\% \pm 3\%$ ) and differentiated enteroids ( $120\% \pm 10\%$ ), verifying the essential role of NKCC1 as a basolateral  $Cl^-$  loader (Figure 9A and B). In addition, the extensive and rapid-onset inhibitory effect of ouabain also occurred in  $HCO_3^-$ -free buffer (Figure 9C). Finally, we found that  $57\% \pm 13\%$  and  $38\% \pm 8\%$  of the forskolin-induced  $\Delta I_{sc}$  in

undifferentiated and differentiated enteroids, respectively, was inhibited by chromanol 293B, indicating the dependence of  $Cl^-$  secretion on basolateral cAMP-activated  $K^+$  channel(s) (Figure 9D and E).<sup>27</sup>

## Discussion

The present study documents the changes in cAMP-stimulated anion secretion and expression of relevant ion transporters during differentiation of normal human duodenal enteroid monolayers, showing the following: (1) similarities with the previous characterization of 3-dimensional human duodenal enteroids, although the changes in expansion medium seem to cause changes in some aspects of the secretory processes<sup>9,22</sup>; (2) that cAMP-stimulated anion secretion occurs in both undifferentiated and differentiated enteroid monolayers, further supporting that ion transport processes in human undifferentiated and differentiated enteroids are more quantitatively than qualitatively different<sup>9,13</sup>; (3) that both undifferentiated and differentiated enteroids perform what appears to be cAMP-stimulated  $Cl^-$  secretion and  $HCO_3^-$  secretion, with  $Cl^-$  secretion being predominant; and (4) that although total anion secretion is much less in differentiated enteroids, the extent of  $HCO_3^-$  secretion is similar in differentiated and undifferentiated enteroids.

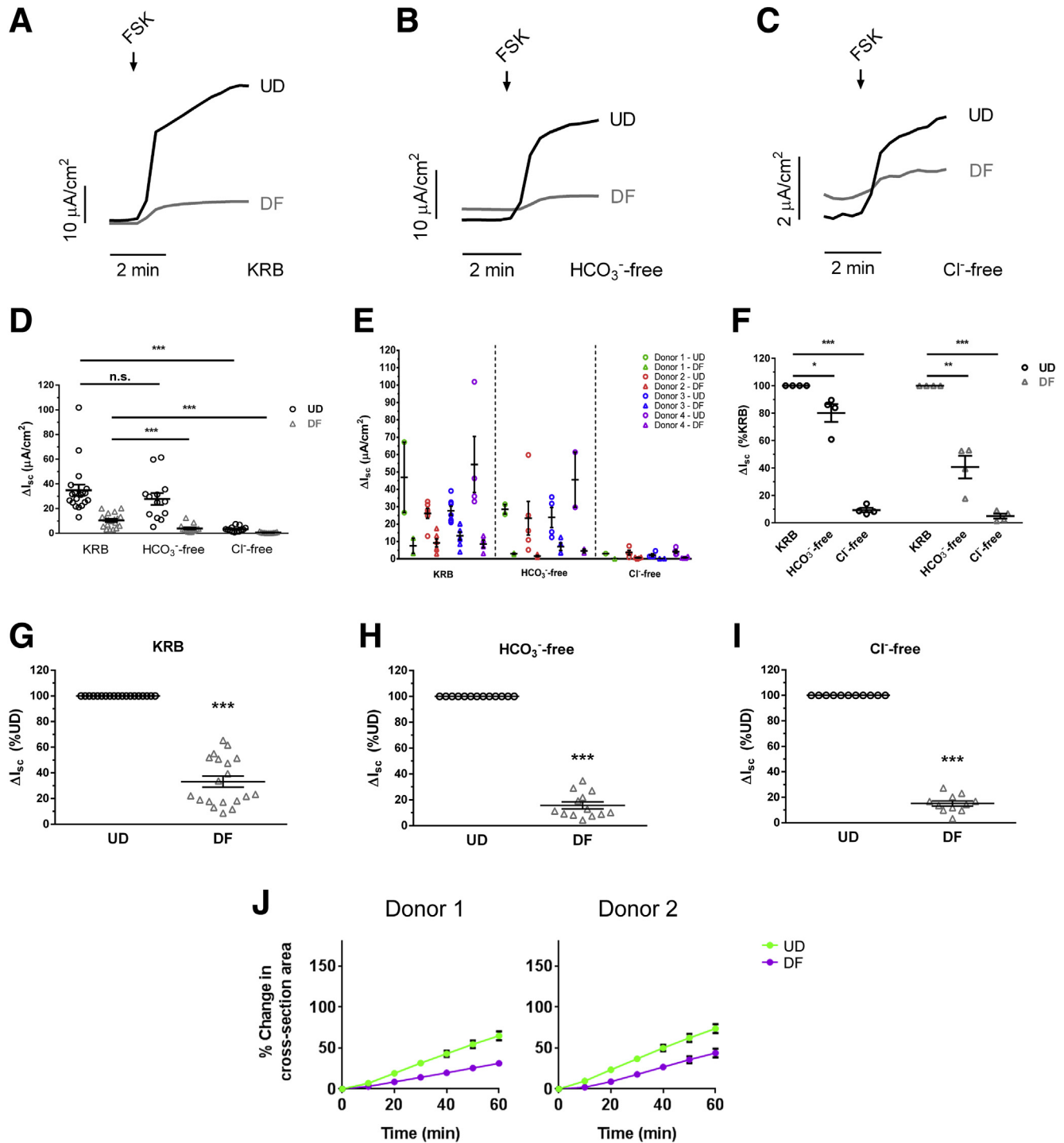
Initially, we showed that the removal of Wnt3A/R-spondin1/SB202190 induced differentiation in duodenal enteroid monolayers, as supported by several phenotypic changes characterized at day 5. Comparison between undifferentiated and differentiated enteroid monolayers also showed several differentiation-related alterations in the expression of multiple ion transporters and carbonic anhydrase isoforms, consistent with the results based on studies of intact human (Turner JR, unpublished data) and animal small intestine.<sup>5</sup> These data support our ability to separately study intestinal epithelial cells that represent crypts and villi using undifferentiated and differentiated enteroids. However, where along the villus our differentiation protocol is modeling is difficult to state given that not all villus cells are differentiated to the same extent, presumably

**Figure 4. (See previous page). Protein expression of selected ion transporters and carbonic anhydrase isoforms in human duodenal enteroid monolayers.** (A) Representative immunoblots showing the protein expression of selected ion transporters and carbonic anhydrase isoforms in undifferentiated (UD) and differentiated (DF) duodenal enteroid monolayers derived from 3 donors. Immunoblotting was performed using 4%–20% gradient gel or 8% gel (for DRA and CFTR). The immunoblot of DRA shows 2 bands representing 2 glycosylated forms of DRA protein, both of which were used for quantitation (see Figure 4C and D). Note that the nitrocellulose membranes were cut into 2 pieces to be blotted with multiple primary antibodies. Proteins that were blotted with rabbit polyclonal antibodies are shown in red, proteins that were blotted with mouse monoclonal antibodies are shown in green. (B) Quantitation showing a significant increase in the protein expression of CA2, DRA, NBCe1, NHE3, and a decrease in CFTR and NKCC1 after differentiation. Calculation was performed using glyceraldehyde-3-phosphate dehydrogenase (GAPDH) as the loading control. \* $P < .05$ , \*\* $P < .01$ , \*\*\* $P < .001$ .  $n = 6$ –13 experiments with paired enteroid monolayers derived from 3–4 donors. (C and D) Protein expression of DRA was studied by immunoblotting using mouse monoclonal primary antibody (sc-376187; Santa Cruz, Dallas, TX). The comparison between wild type HEK cells (lacking DRA mRNA and protein) and HEK cells with transient transfection of 3xFLAG-DRA showed 2 potential DRA bands. A deglycosylation study was performed using PNGase F (New England Biolabs, Ipswich, MA) according to the manufacturer's protocols, showing the 2 bands represent 2 glycosylated forms of DRA protein in differentiated duodenal enteroid monolayers (endogenous DRA expression) and HEK cells with transient transfection of 3xFLAG-DRA (exogenous DRA expression).

continuing to differentiate as they move from the base of villus to the tip. Moreover, data are lacking that show the differentiation state and expression of transport proteins in epithelial cells at multiple positions along the human intestinal villus. Similarly, although the crypt base has LGR5-positive stem cells, Paneth cells, and transit-amplifying cells that proliferate, it is likely that cells of multiple states of differentiation are present, particularly at the upper crypt. Importantly, it is

not yet known where in the crypt the anion secretory cells appear.

A major contribution of this study is the identification of the transport processes and cell populations that contribute to small intestinal anion secretion stimulated by increased intracellular cAMP. Although the functional relevance of enteroids to understanding human intestinal ion transport physiology has been shown by several previous studies,<sup>9,24</sup> the characterization of human intestinal anion secretory



processes remains incomplete. In the present study, we defined active electrogenic anion secretion stimulated by forskolin in human duodenal enteroid monolayers by the Ussing chamber/voltage-current clamp technique. Specifically, this includes cAMP-stimulated  $\text{Cl}^-$  secretion ( $\text{HCO}_3^-$ -independent and  $\text{HCO}_3^-$ -dependent) and  $\text{HCO}_3^-$  secretion ( $\text{Cl}^-$ -independent and  $\text{Cl}^-$ -dependent). It is important to point out that only electrogenic ion transport is defined by the approach of measuring  $I_{sc}$ ; this did not allow us to specifically quantitate the electroneutral  $\text{Cl}^-$ -dependent  $\text{HCO}_3^-$  secretion that is provided by an apical anion exchanger, such as DRA, which exchanges  $\text{Cl}^-$  that is secreted by CFTR for intracellular  $\text{HCO}_3^-$ , and that together with the linked CFTR-related  $\text{Cl}^-$  secretion is an overall electrogenic process.<sup>28</sup> Similarly, the specific contribution of  $\text{HCO}_3^-$ -dependent  $\text{Cl}^-$  secretion, which includes the putative activated DRA stimulation of CFTR activity, could not be determined,<sup>29,30</sup> nor is it known if it occurs in intact mammalian small intestine. In addition, the current study was not able to simultaneously quantitate the amount of active  $\text{HCO}_3^-$  transport, given that our available equipment could not accomplish simultaneous pH titration and short-circuiting. In addition, although we have found many similarities in cAMP-stimulated secretion between enteroids derived from duodenum and jejunum, the findings of the current study in duodenal enteroids may not be completely extrapolated to other small intestinal segments given the special functions of each segment.

cAMP-stimulated anion secretion was present in both the crypt-like-undifferentiated enteroids and the villus-like-differentiated enteroids with the following characteristics. First, the magnitude of forskolin-stimulated anion secretion in differentiated enteroids was approximately 33% of that in undifferentiated enteroids. Second, a reduction in the magnitude of forskolin-induced  $\Delta I_{sc}$  was

observed in both undifferentiated and differentiated enteroids after the removal of extracellular  $\text{Cl}^-$ , presumably owing to loss of  $\text{Cl}^-$  secretion and also  $\text{Cl}^-$ -dependent  $\text{HCO}_3^-$  secretion. Similarly, the removal of extracellular  $\text{HCO}_3^-/\text{CO}_2$ , which causes loss of  $\text{HCO}_3^-$  secretion and  $\text{HCO}_3^-$ -dependent  $\text{Cl}^-$  secretion, resulted in reduced magnitude of forskolin-induced  $\Delta I_{sc}$ , but this was modest compared with that with extracellular  $\text{Cl}^-$  removal. Similar effects of extracellular anion removal also were found in mouse duodenum.<sup>31,32</sup> Although the cAMP-stimulated anion secretion in the absence of extracellular  $\text{Cl}^-$  or  $\text{HCO}_3^-/\text{CO}_2$  does not represent the entire  $\text{HCO}_3^-$  or  $\text{Cl}^-$  secretion, this method of extracellular anion removal at least allowed us to confirm the dependency of cAMP-stimulated anion secretion on extracellular anions. Third,  $\text{Cl}^-$  secretion, primarily defined as the bumetanide-sensitive component of forskolin-induced  $\Delta I_{sc}$ , makes up the bulk of anion secretion in undifferentiated enteroids and a significant part in differentiated enteroids. Specifically, 75% of the forskolin-induced  $\Delta I_{sc}$  was inhibited by bumetanide in undifferentiated enteroids and 44% in differentiated enteroids. This is consistent with the *in vivo* observation that bumetanide inhibited a large part of forskolin-induced  $\Delta I_{sc}$  without affecting bicarbonate secretion in mouse duodenum.<sup>33</sup> Fourth, a bumetanide-insensitive component of forskolin-induced  $\Delta I_{sc}$  was observed in both undifferentiated and differentiated enteroids. This residual component is either  $\text{Cl}^-$  secretion dependent on another bumetanide-insensitive basolateral  $\text{Cl}^-$  uptake pathway or  $\text{HCO}_3^-$  secretion. The former has not been identified in the small intestine. Also, although the basolateral anion exchanger AE2, which is present similarly in undifferentiated and differentiated enteroids, could provide such a transport pathway,<sup>25,33</sup> the lack of effect on forskolin-induced  $\Delta I_{sc}$  by blocking AE2 with SITS suggests it unlikely to be involved. Of note, this bumetanide-insensitive

**Figure 5.** (See *previous page*). **cAMP-stimulated electrogenic anion secretion in human duodenal enteroid monolayers.** (A–C) Representative traces showing forskolin-induced  $\Delta I_{sc}$  arising from undifferentiated (UD) and differentiated (DF) duodenal enteroid monolayers in (A) KRB buffer, (B)  $\text{HCO}_3^-$ -free buffer, and (C)  $\text{Cl}^-$ -free buffer. In all experiments, forskolin (10  $\mu\text{mol/L}$ ) was added to the basolateral side to induce anion secretion. (D) Scatter plots showing the magnitude of forskolin-induced  $\Delta I_{sc}$  for undifferentiated enteroids and differentiated enteroids in multiple buffer conditions. Each plot represents the result of a single experiment ( $n = 1\text{--}3$  enteroid monolayers). Statistical analysis was performed using an unpaired *t* test.  $***P < .001$ .  $n = 11\text{--}19$  experiments with paired enteroid monolayers derived from 4 donors. (E) Scatter plots showing the individual data of each enteroid line from Figure 4D. Each plot represents the result of a single experiment ( $n = 1\text{--}3$  enteroid monolayers). Each color represents a single enteroid line derived from an individual donor. Note the moderate variability in the magnitude of forskolin-induced  $\Delta I_{sc}$  between enteroid lines derived from different donors and between experiments within each single enteroid line. The *horizontal lines* are the means, and the standard error bars show the experimental variability within each single enteroid line.  $n = 11\text{--}19$  experiments with paired enteroid monolayers derived from 4 donors. (F) Quantitative analysis comparing the magnitude of forskolin-induced  $\Delta I_{sc}$  in  $\text{HCO}_3^-$ -free buffer and  $\text{Cl}^-$ -free buffer with that in KRB buffer (set as 100%). In both undifferentiated and differentiated enteroids, there was a significant reduction in forskolin-induced  $\Delta I_{sc}$  after the removal of extracellular  $\text{HCO}_3^-/\text{CO}_2$  and an even more pronounced reduction after the removal of extracellular  $\text{Cl}^-$ .  $*P < .05$ ,  $**P < .01$ ,  $***P < .001$ .  $n = 4$  enteroid lines derived from 4 separate donors (the results were first analyzed within each single enteroid line and the averages of each enteroid line subsequently were combined for statistical analysis considering the total number of enteroid lines as the sample size). (G–I) Quantitation showing a significantly lower magnitude of forskolin-induced  $\Delta I_{sc}$  in differentiated enteroids compared with undifferentiated enteroids (set as 100%) in (G) KRB buffer, (H)  $\text{HCO}_3^-$ -free buffer, and (I)  $\text{Cl}^-$ -free buffer.  $***P < .001$ .  $n = 11\text{--}19$  experiments with paired enteroid monolayers derived from 4 donors for each buffer condition. (J) Representative time-course changes of forskolin-induced swelling in 3-dimensional duodenal enteroids derived from 2 donors. Forskolin-induced swelling assay was performed as previously reported,<sup>9</sup> and in contrast to our previous finding, the current study found greater forskolin-induced swelling in undifferentiated enteroids than differentiated enteroids, which likely resulted from the changes in the composition of expansion medium, with one of the major changes being the removal of nicotamide.<sup>22</sup>

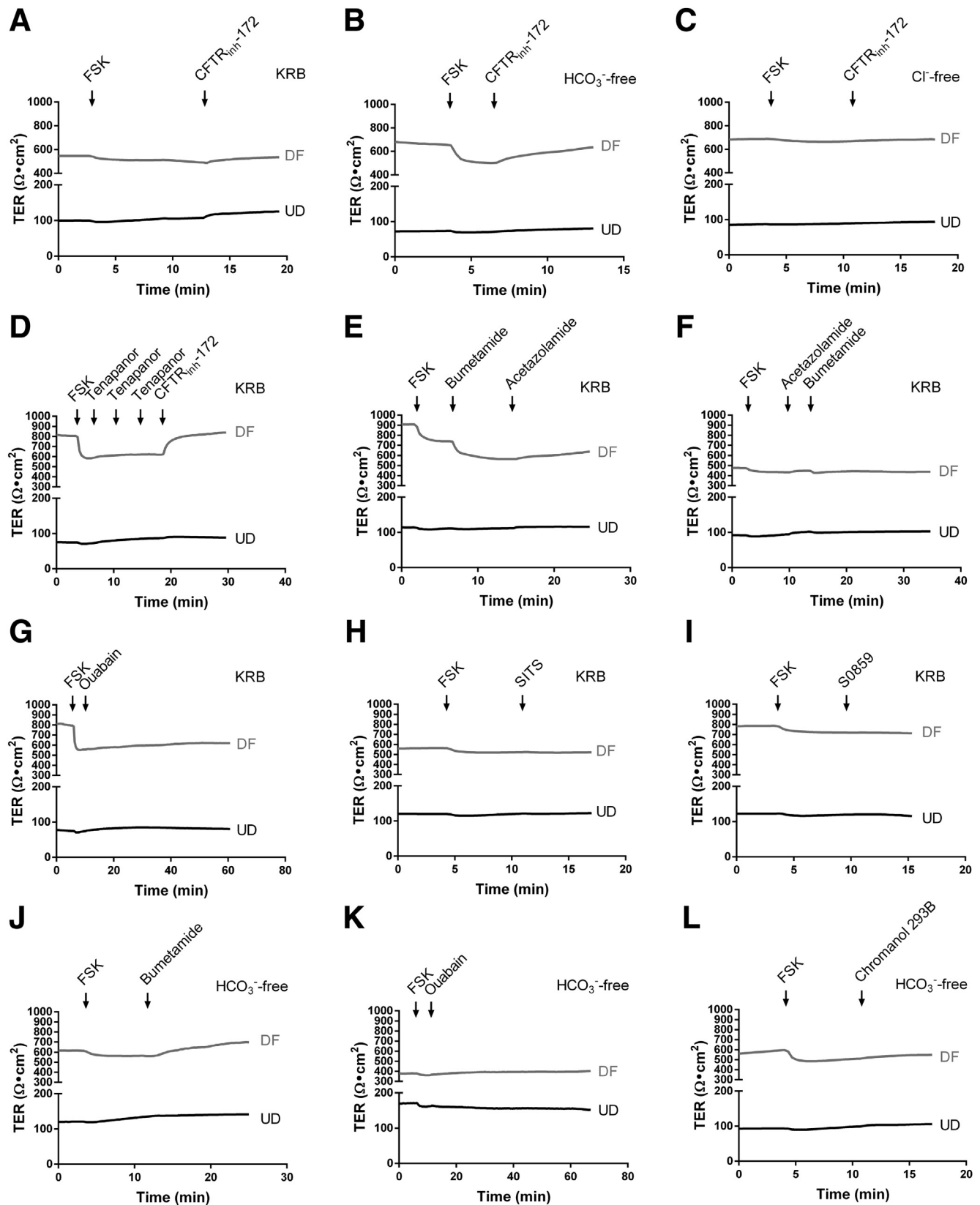


**Figure 6.** Effects of selected compounds on TER. Representative traces showing the effects of selective compounds on TER. TER was recorded at the same time as short-circuit current was studied. (A–C) Corresponds to Figure 7A–C, (D) corresponds to Figure 7F, (E and F) corresponds to Figure 8A and B; (G–I) corresponds to Figure 8F–H, (J) corresponds to Figure 9A, and (K and L) corresponds to Figure 9C and D.

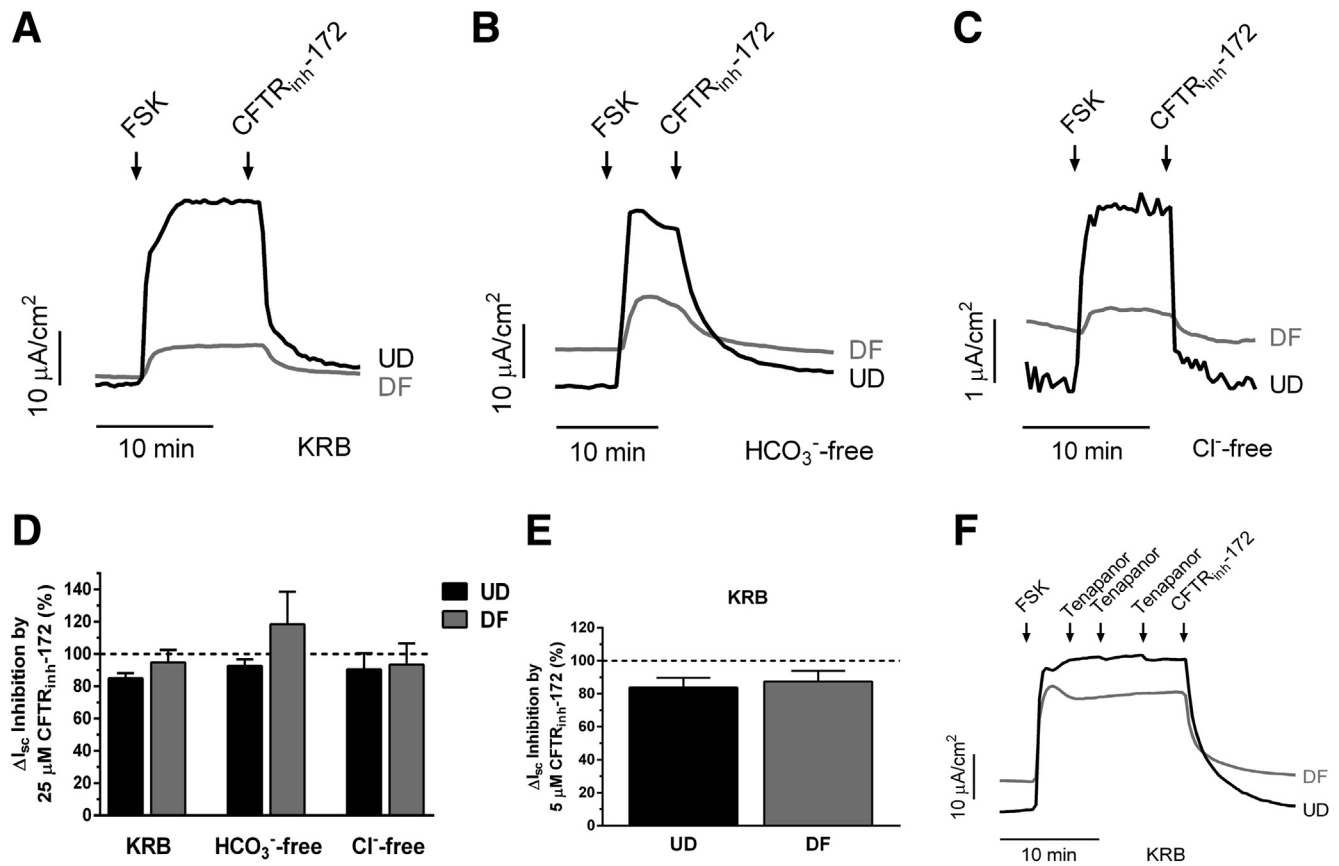


**Figure 7. Functional involvement of apical ion transporters in cAMP-stimulated electrogenic anion secretion.** (A–C) Representative traces showing the inhibitory effect of CFTR<sub>inh</sub>-172 (25 μmol/L on the apical side) on forskolin-induced  $\Delta I_{sc}$  arising from undifferentiated (UD) and differentiated (DF) enteroid monolayers in (A) KRB buffer, (B) HCO<sub>3</sub><sup>-</sup>-free buffer, and (C) Cl<sup>-</sup>-free buffer. (D) Quantitation showing CFTR<sub>inh</sub>-172 (25 μmol/L on the apical side) inhibited the majority of forskolin-induced  $\Delta I_{sc}$  in both undifferentiated and differentiated enteroids in all buffer conditions. *n* = 3–5 experiments with paired enteroid monolayers derived from 2–3 donors for each buffer condition. (E) Quantitation showing a lower dose of CFTR<sub>inh</sub>-172 (5 μmol/L on the apical side) also inhibited the majority of forskolin-induced  $\Delta I_{sc}$  in both undifferentiated and differentiated enteroids in KRB buffer. *n* = 3 experiments with paired enteroid monolayers derived from 2 donors. (F) A representative trace showing the insensitivity of forskolin-induced  $\Delta I_{sc}$  to tenapanor in KRB buffer. The cumulative concentration of tenapanor on the apical side after each addition was 0.1 μmol/L, 0.5 μmol/L, and 1 μmol/L. This experiment was repeated at least 3 times using paired enteroid monolayers derived from 2 donors, and similar results were found in each experiment.

component was seen only in KRB buffer that contains HCO<sub>3</sub><sup>-</sup>/CO<sub>2</sub>; it was not observed in HCO<sub>3</sub><sup>-</sup>-free buffer, suggesting that it involves HCO<sub>3</sub><sup>-</sup> secretion. In fact, a similar bumetanide-insensitive component also was found in mouse duodenum only when extracellular HCO<sub>3</sub><sup>-</sup> was present.<sup>31</sup> That this was likely to be HCO<sub>3</sub><sup>-</sup> secretion was supported further by its sensitivity to acetazolamide, which has been shown to inhibit basal and stimulated HCO<sub>3</sub><sup>-</sup> secretion in intact human/animal duodenum.<sup>34–36</sup> Taken together, these results show the similarity of human duodenal enteroid monolayers and intact human/mouse duodenum in many aspects of cAMP-stimulated Cl<sup>-</sup> and HCO<sub>3</sub><sup>-</sup> secretion.

As we proposed previously,<sup>13</sup> that forskolin-induced  $\Delta I_{sc}$  is detectable in villus-like-differentiated enteroids suggests anion secretion is not strictly confined to crypts, although a significant quantitative difference exists between

differentiated and undifferentiated enteroids. The lesser anion secretion in differentiated enteroids seems to be caused largely by the reduction in Cl<sup>-</sup> secretion, which is related to the reduced expression of CFTR, NKCC1 and KCNE3, all of which are known to be necessary for cAMP-stimulated Cl<sup>-</sup> secretion. Interestingly, several ion transporters and carbonic anhydrase isoforms that are involved in HCO<sub>3</sub><sup>-</sup> secretion, including DRA, NBCe1, CA2, and CA4, were increased in differentiated enteroids. These changes may explain that the absolute amount of forskolin-induced  $\Delta I_{sc}$  that was inhibited by acetazolamide, which represents a component of HCO<sub>3</sub><sup>-</sup> secretion, was similar between undifferentiated and differentiated enteroids despite a significant reduction in CFTR expression in the latter. Further studies are needed to determine whether these changes in expression lead to increased DRA-related Cl<sup>-</sup>-dependent

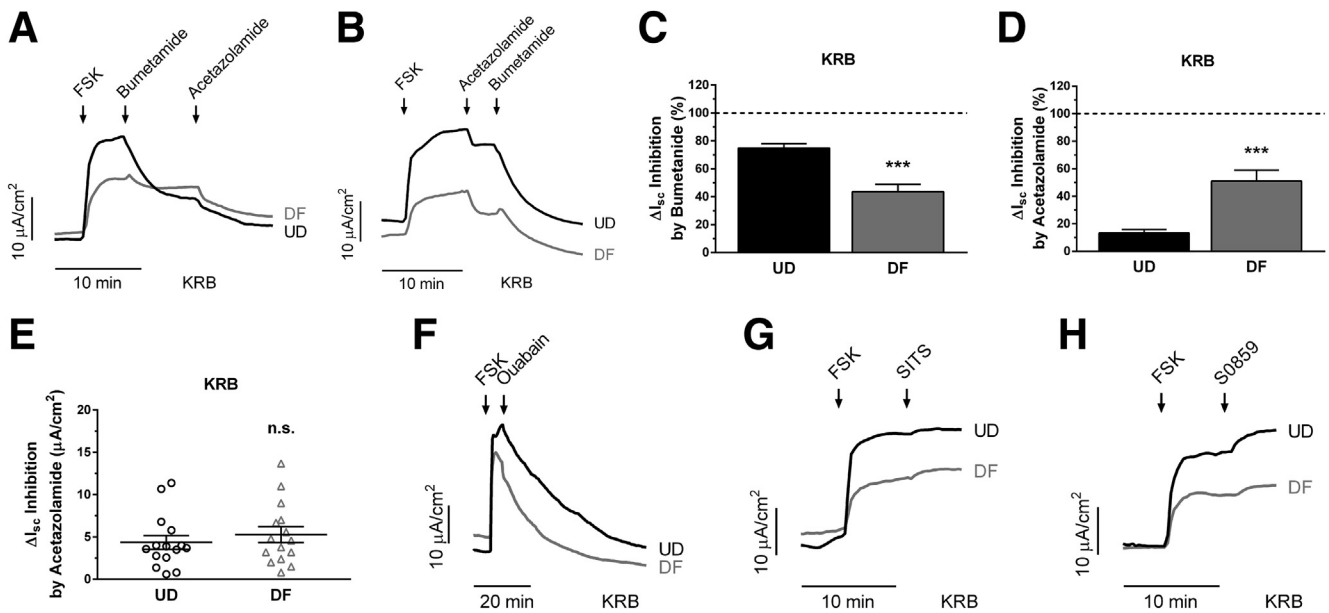


**Figure 8. Functional involvement of basolateral ion transporters and carbonic anhydrase(s) in cAMP-stimulated electrogenic anion secretion.** (A and B) Representative traces showing forskolin-induced  $\Delta I_{sc}$  arising from undifferentiated (UD) and differentiated (DF) enteroid monolayers was sensitive to bumetanide (100  $\mu\text{mol/L}$  on the basolateral side) and acetazolamide (250  $\mu\text{mol/L}$  on both apical and basolateral sides) in KRB buffer. The combination of the 2 compounds abolished forskolin-induced  $\Delta I_{sc}$  despite their order. (C and D) Quantitation showing the percentage of forskolin-induced  $\Delta I_{sc}$  that was inhibited by (C) bumetanide and (D) acetazolamide in KRB buffer. Undifferentiated enteroids showed a relatively higher sensitivity to bumetanide than to acetazolamide, whereas differentiated enteroids showed a relatively higher sensitivity to acetazolamide than to bumetanide. The differences between undifferentiated and differentiated enteroids in their sensitivity to bumetanide and acetazolamide were statistically significant ( $***P < .001$ ).  $n = 15$  experiments with paired enteroid monolayers derived from 4 donors. (E) Quantitation showing the absolute reduction in the magnitude of forskolin-induced  $\Delta I_{sc}$  by acetazolamide in KRB buffer. There was no statistical difference between undifferentiated enteroids and differentiated enteroids.  $n = 15$  experiments with paired enteroid monolayers derived from 4 donors. (F and G) Representative traces showing the effects of ouabain (F, 100  $\mu\text{mol/L}$  on the basolateral side), SITS (G, 1  $\text{mmol/L}$  on the basolateral side), and S0859 (H, 30  $\mu\text{mol/L}$  on the basolateral side) on forskolin-induced  $\Delta I_{sc}$  in KRB buffer. These experiments were repeated at least 3 times using paired enteroid monolayers derived from 2 to 3 donors, and similar results were found in each experiment.

$\text{HCO}_3^-$  secretion in differentiated enteroids, a process that was not determined by the Ussing chamber/voltage-current clamp technique used in this study.

The present study allowed further dissection of the contribution of specific transporters to cAMP-stimulated anion secretion in duodenal enteroids. On the apical surface, CFTR was found to be necessary for both  $\text{Cl}^-$  and  $\text{HCO}_3^-$  secretion because CFTR<sub>inh</sub>-172 abolished the entire forskolin-induced  $\Delta I_{sc}$  in the presence and absence of extracellular  $\text{Cl}^-$  and  $\text{HCO}_3^-/\text{CO}_2$  in differentiated as well as undifferentiated enteroids. Thus, CFTR is the major apical transporter for all duodenal cAMP-stimulated anion secretion and no other  $\text{Cl}^-$  channel seems to contribute significantly, unless that contribution is indirect and involves CFTR. Similarly, there appears no role for NHE3 in cAMP-stimulated anion secretion because forskolin-induced  $\Delta I_{sc}$  was not altered by tenapanor. However, NHE3 still could have a role in electroneutral  $\text{HCO}_3^-$  secretion,<sup>28,31</sup> which could not be quantitated in the current study. Any specific role for DRA and PAT-1 could not be evaluated in this study, although they are

likely to contribute to cAMP-stimulated anion secretion through their interaction with CFTR.<sup>28,37</sup>

In terms of the basolateral transporters participating in cAMP-stimulated  $\text{Cl}^-$  secretion, our results confirmed NKCC1 as the essential basolateral  $\text{Cl}^-$  loader and the necessary contributions of cAMP-activated  $\text{K}^+$  channel(s) and  $\text{Na}^+/\text{K}^+$ -ATPase.<sup>32,38,39</sup> As for cAMP-stimulated  $\text{HCO}_3^-$  secretion, there are 2 potential pathways that could supply  $\text{HCO}_3^-$  for apical extrusion. One is a  $\text{Na}^+/\text{HCO}_3^-$  co-transporter that interacts with NHE1 to mediate  $\text{HCO}_3^-$  uptake across the basolateral membrane.<sup>36</sup> Our study did not provide any evidence for the involvement of NBCs because a specific inhibitor of the NBC family (S0859) had no significant inhibitory effect but rather a small stimulatory effect on forskolin-induced  $\Delta I_{sc}$ . A similar transient stimulatory effect of S0859 on forskolin-induced  $\Delta I_{sc}$  also was seen in bronchial epithelial cells, which could be inhibited by calcium-activated chloride channel (CaCC) inhibitor.<sup>40</sup> The second source of  $\text{HCO}_3^-$  is the production of intracellular  $\text{HCO}_3^-$  by carbonic anhydrase(s), the contribution of which is supported by

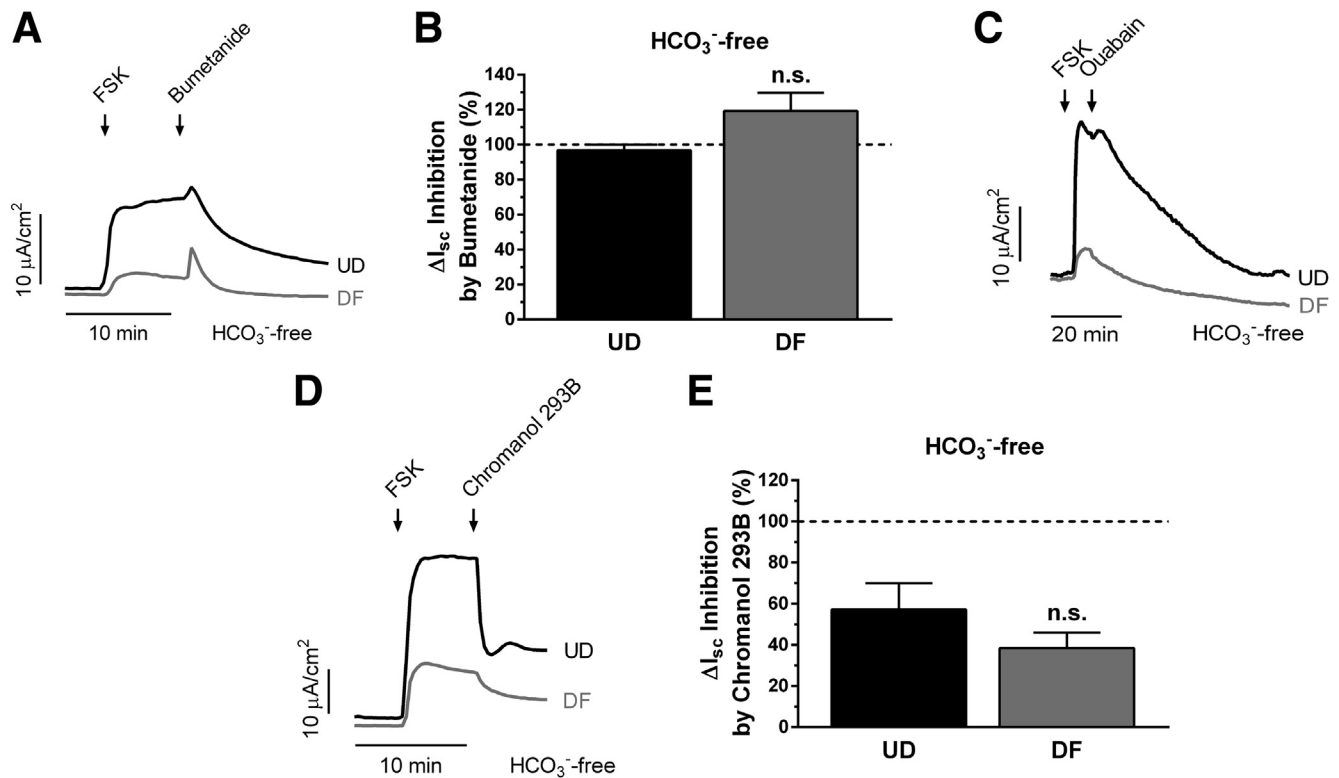


**Figure 9. Functional involvement of basolateral transporters in cAMP-stimulated electrogenic  $\text{Cl}^-$  secretion.** (A and B) A representative trace and quantitative analysis showing the inhibitory effect of bumetanide ( $100 \mu\text{mol/L}$  on the basolateral side) on forskolin-induced  $\Delta I_{\text{sc}}$  arising from undifferentiated (UD) and differentiated (DF) enteroid monolayers in  $\text{HCO}_3^-$ -free buffer.  $n = 4$  experiments with paired enteroid monolayers derived from 3 donors. (C) A representative trace showing the inhibitory effect of ouabain ( $100 \mu\text{mol/L}$  on the basolateral side) on forskolin-induced  $\Delta I_{\text{sc}}$  in  $\text{HCO}_3^-$ -free buffer. This experiment was repeated at least 3 times using paired enteroid monolayers derived from 2 donors, and similar results were found in each experiment. (D and E) A representative trace and quantitative analysis showing the inhibitory effect of chromanol 293B ( $10 \mu\text{mol/L}$  on the basolateral side) on forskolin-induced  $\Delta I_{\text{sc}}$  in  $\text{HCO}_3^-$ -free buffer.  $n = 5$  experiments with paired enteroid monolayers derived from 2 donors.

the inhibitory effect of acetazolamide on  $\text{HCO}_3^-$  secretion, as shown by multiple studies.<sup>34–36</sup> In the current study, an acetazolamide-sensitive component was present in cAMP-stimulated anion secretion, indicating the requirement for carbonic anhydrase(s) in  $\text{HCO}_3^-$  secretion. However, the specific carbonic anhydrase isoform was not identified. Two isoforms were up-regulated significantly with differentiation in duodenal enteroids; CA2 is thought to be the major enzyme involved in intracellular  $\text{HCO}_3^-$  production, and CA4 is expressed only in differentiated enteroids and is reported to interact with CFTR and facilitate  $\text{CO}_2$  influx.<sup>41,42</sup>

In conclusion, this study describes some of the molecular basis of cAMP-stimulated anion secretion in normal human duodenal enteroid monolayers and compares the ion transport processes taking part in anion secretion in crypt-like-undifferentiated enteroids and villus-like-differentiated enteroids. We suggest that human enteroid monolayers are a useful tool to study multiple physiological and pathophysiological models of intestinal anion secretion, including the chloride and bicarbonate components, as well as those that are caused

separately by crypt-like and villus-like epithelial cells of human small intestine.

## References

1. Field M. Intestinal ion transport and the pathophysiology of diarrhea. *J Clin Invest* 2003;111:931–943.
2. Ikpa PT, Sleddens HF, Steinbrecher KA, Peppelenbosch MP, de Jonge HR, Smits R, Bijvelds MJ. Guanylin and uroguanylin are produced by mouse intestinal epithelial cells of columnar and secretory lineage. *Histochem Cell Biol* 2016;146:445–455.
3. Ledford H. Translational research: 4 ways to fix the clinical trial. *Nature* 2011;477:526–528.
4. De Jonge HR. The response of small intestinal villous and crypt epithelium to cholera toxin in rat and guinea pig. Evidence against a specific role of the crypt cells in cholera toxin-induced secretion. *Biochim Biophys Acta* 1975;381:128–143.
5. Jakab RL, Collaco AM, Ameen NA. Physiological relevance of cell-specific distribution patterns of CFTR, NKCC1, NBCe1, and NHE3 along the crypt-villus axis in

- the intestine. *Am J Physiol Gastrointest Liver Physiol* 2011;300:G82–G98.
6. Kockerling A, Fromm M. Origin of cAMP-dependent Cl<sup>-</sup> secretion from both crypts and surface epithelia of rat intestine. *Am J Physiol* 1993;264:C1294–C1301.
  7. McNicholas CM, Brown CD, Turnberg LA. Na-K-Cl cotransport in villus and crypt cells from rat duodenum. *Am J Physiol* 1994;267:G1004–G1011.
  8. Yin J, Tse CM, Cha B, Sarker R, Zhu XC, Walentinsson A, Greasley PJ, Donowitz M. A common NHE3 single nucleotide polymorphism has normal function and sensitivity to regulatory ligands. *Am J Physiol Gastrointest Liver Physiol* 2017;313:G129–G137.
  9. Foulke-Abel J, In J, Yin J, Zachos NC, Kovbasnjuk O, Estes MK, de Jonge H, Donowitz M. Human enteroids as a model of upper small intestinal ion transport physiology and pathophysiology. *Gastroenterology* 2016;150:638–649 e8.
  10. Stewart CP, Turnberg LA. A microelectrode study of responses to secretagogues by epithelial cells on villus and crypt of rat small intestine. *Am J Physiol* 1989;257:G334–G343.
  11. Sato T, Stange DE, Ferrante M, Vries RG, Van Es JH, Van den Brink S, Van Houdt WJ, Pronk A, Van Gorp J, Siersema PD, Clevers H. Long-term expansion of epithelial organoids from human colon, adenoma, adenocarcinoma, and Barrett's epithelium. *Gastroenterology* 2011;141:1762–1772.
  12. Sato T, Vries RG, Snippert HJ, van de Wetering M, Barker N, Stange DE, van Es JH, Abo A, Kujala P, Peters PJ, Clevers H. Single Lgr5 stem cells build crypt-villus structures in vitro without a mesenchymal niche. *Nature* 2009;459:262–265.
  13. Yu H, Hasan NM, In JG, Estes MK, Kovbasnjuk O, Zachos NC, Donowitz M. The contributions of human mini-intestines to the study of intestinal physiology and pathophysiology. *Annu Rev Physiol* 2017;79:291–312.
  14. Ettayebi K, Crawford SE, Murakami K, Broughman JR, Karandikar U, Tenge VR, Neill FH, Blutt SE, Zeng XL, Qu L, Kou B, Opekun AR, Burrin D, Graham DY, Ramani S, Atmar RL, Estes MK. Replication of human noroviruses in stem cell-derived human enteroids. *Science* 2016;353:1387–1393.
  15. Noel G, Baetz NW, Staab JF, Donowitz M, Kovbasnjuk O, Pasetti MF, Zachos NC. A primary human macrophage-enteroid co-culture model to investigate mucosal gut physiology and host-pathogen interactions. *Sci Rep* 2017;7:45270.
  16. In J, Foulke-Abel J, Zachos NC, Hansen AM, Kaper JB, Bernstein HD, Halushka M, Blutt S, Estes MK, Donowitz M, Kovbasnjuk O. Enterohemorrhagic reduce mucus and intermicrovillar bridges in human stem cell-derived colonoids. *Cell Mol Gastroenterol Hepatol* 2016;2:48–62 e3.
  17. Sato T, Clevers H. Primary mouse small intestinal epithelial cell cultures. *Methods Mol Biol* 2013;945:319–328.
  18. Heijmans J, van Lidth de Jeude JF, Koo BK, Rosekrans SL, Wielenga MC, van de Wetering M, Ferrante M, Lee AS, Onderwater JJ, Paton JC, Paton AW, Mommaas AM, Kodach LL, Hardwick JC, Hommes DW, Clevers H, Muncan V, van den Brink GR. ER stress causes rapid loss of intestinal epithelial stemness through activation of the unfolded protein response. *Cell Rep* 2013;3:1128–1139.
  19. Clarke LL. A guide to Ussing chamber studies of mouse intestine. *Am J Physiol Gastrointest Liver Physiol* 2009;296:G1151–G1166.
  20. Thompson CA, Wojta K, Pulakanti K, Rao S, Dawson P, Battle MA. GATA4 is sufficient to establish jejunal versus ileal identity in the small intestine. *Cell Mol Gastroenterol Hepatol* 2017;3:422–446.
  21. Middendorp S, Schneeberger K, Wiegerinck CL, Mokry M, Akkerman RD, van Wijngaarden S, Clevers H, Nieuwenhuis EE. Adult stem cells in the small intestine are intrinsically programmed with their location-specific function. *Stem Cells* 2014;32:1083–1091.
  22. Fujii M, Matano M, Nanki K, Sato T. Efficient genetic engineering of human intestinal organoids using electroporation. *Nat Protoc* 2015;10:1474–1485.
  23. Tang L, Fatehi M, Linsdell P. Mechanism of direct bicarbonate transport by the CFTR anion channel. *J Cyst Fibros* 2009;8:115–121.
  24. Cil O, Phuan PW, Gillespie AM, Lee S, Tradtrantip L, Yin J, Tse M, Zachos NC, Lin R, Donowitz M, Verkman AS. Benzopyrimido-pyrrolo-oxazine-dione CFTR inhibitor (R)-BPO-27 for antisecretory therapy of diarrheas caused by bacterial enterotoxins. *FASEB J* 2017;31:751–760.
  25. Gawenis LR, Bradford EM, Alper SL, Prasad V, Shull GE. AE2 Cl<sup>-</sup>/HCO<sub>3</sub><sup>-</sup> exchanger is required for normal cAMP-stimulated anion secretion in murine proximal colon. *Am J Physiol Gastrointest Liver Physiol* 2010;298:G493–G503.
  26. Ch'en FF, Villafuerte FC, Swietach P, Cobden PM, Vaughan-Jones RD. S0859, an N-cyanosulphonamide inhibitor of sodium-bicarbonate cotransport in the heart. *Br J Pharmacol* 2008;153:972–982.
  27. Mall M, Kunzelmann K, Hipper A, Busch AE, Greger R. cAMP stimulation of CFTR-expressing *Xenopus* oocytes activates a chromanol-inhibitable K<sup>+</sup> conductance. *Pflugers Arch* 1996;432:516–522.
  28. Singh AK, Riederer B, Chen M, Xiao F, Krabbenhöft A, Engelhardt R, Nylander O, Soleimani M, Seidler U. The switch of intestinal Slc26 exchangers from anion absorptive to HCO<sub>3</sub><sup>-</sup> secretory mode is dependent on CFTR anion channel function. *Am J Physiol Cell Physiol* 2010;298:C1057–C1065.
  29. Shan J, Liao J, Huang J, Robert R, Palmer ML, Fahrenkrug SC, O'Grady SM, Hanrahan JW. Bicarbonate-dependent chloride transport drives fluid secretion by the human airway epithelial cell line Calu-3. *J Physiol* 2012;590:5273–5297.
  30. Hong JH, Yang D, Shcheynikov N, Ohana E, Shin DM, Muallem S. Convergence of IRBIT, phosphatidylinositol (4,5) bisphosphate, and WNK/SPAK kinases in regulation of the Na<sup>+</sup>-HCO<sub>3</sub><sup>-</sup> cotransporters family. *Proc Natl Acad Sci U S A* 2013;110:4105–4110.
  31. Clarke LL, Stien X, Walker NM. Intestinal bicarbonate secretion in cystic fibrosis mice. *JOP* 2001;2:263–267.

32. Seidler U, Blumenstein I, Kretz A, Viellard-Baron D, Rossmann H, Colledge WH, Evans M, Ratcliff R, Gregor M. A functional CFTR protein is required for mouse intestinal cAMP-, cGMP- and Ca<sup>2+</sup>-dependent HCO<sub>3</sub><sup>-</sup> secretion. *J Physiol* 1997;505:411–423.
33. Walker NM, Flagella M, Gawenis LR, Shull GE, Clarke LL. An alternate pathway of cAMP-stimulated Cl<sup>-</sup> secretion across the NKCC1-null murine duodenum. *Gastroenterology* 2002;123:531–541.
34. Knutson TW, Koss MA, Hogan DL, Isenberg JI, Knutson L. Acetazolamide inhibits basal and stimulated HCO<sub>3</sub><sup>-</sup> secretion in the human proximal duodenum. *Gastroenterology* 1995;108:102–107.
35. Muallem R, Reimer R, Odes HS, Schwenk M, Beil W, Sewing KF. Role of carbonic anhydrase in basal and stimulated bicarbonate secretion by the guinea pig duodenum. *Dig Dis Sci* 1994;39:1078–1084.
36. Jacob P, Christiani S, Rossmann H, Lamprecht G, Viellard-Baron D, Müller R, Gregor M, Seidler U. Role of Na<sup>+</sup>HCO<sub>3</sub><sup>-</sup> cotransporter NBC1, Na<sup>+</sup>/H<sup>+</sup> exchanger NHE1, and carbonic anhydrase in rabbit duodenal bicarbonate secretion. *Gastroenterology* 2000;119:406–419.
37. Walker NM, Simpson JE, Brazill JM, Gill RK, Dudeja PK, Schweinfest CW, Clarke LL. Role of down-regulated in adenoma anion exchanger in HCO<sub>3</sub><sup>-</sup> secretion across murine duodenum. *Gastroenterology* 2009;136:893–901.
38. Preston P, Wartosch L, Günzel D, Fromm M, Kongsuphol P, Ousingsawat J, Kunzelmann K, Barhanin J, Warth R, Jentsch TJ. Disruption of the K<sup>+</sup> channel beta-subunit KCNE3 reveals an important role in intestinal and tracheal Cl<sup>-</sup> transport. *J Biol Chem* 2010;285:7165–7175.
39. Seidler U, Bachmann O, Jacob P, Christiani S, Blumenstein I, Rossmann H. Na<sup>+</sup>/HCO<sub>3</sub><sup>-</sup> cotransport in normal and cystic fibrosis intestine. *JOP* 2001;2:247–256.
40. Gorrieri G, Scudieri P, Caci E, Schiavon M, Tomati V, Sirci F, Napolitano F, Carrella D, Gianotti A, Musante I, Favia M, Casavola V, Guerra L, Rea F, Ravazzolo R, Di Bernardo D, Galletta LJ. Goblet cell hyperplasia requires high bicarbonate transport to support mucin release. *Sci Rep* 2016;6:36016.
41. Fanjul M, Salvador C, Alvarez L, Cantet S, Hollande E. Targeting of carbonic anhydrase IV to plasma membranes is altered in cultured human pancreatic duct cells expressing a mutated ( $\Delta$ F508) CFTR. *Eur J Cell Biol* 2002;81:437–447.
42. Musa-Aziz R, Occhipinti R, Boron WF. Evidence from simultaneous intracellular- and surface-pH transients that carbonic anhydrase IV enhances CO<sub>2</sub> fluxes across *Xenopus* oocyte plasma membranes. *Am J Physiol Cell Physiol* 2014;307:C814–C840.

---

Received July 14, 2017. Accepted February 5, 2018.

#### Correspondence

Address correspondence to: Mark Donowitz, MD, Johns Hopkins University School of Medicine, 720 Rutland Avenue, 925 Ross Research Building, Baltimore, Maryland 21205. e-mail: [mdonowitz@jhmi.edu](mailto:mdonowitz@jhmi.edu); fax: (410) 955-9677.

#### Acknowledgments

The authors are grateful to Denise Chesner, MS, Janet Staab, PhD, Michele Doucet, MS (Johns Hopkins University, Baltimore, MD) for their assistance in cell culture and media preparation. The authors also thank Ardelyx, Inc (Fremont, CA) for providing tenapanor.

#### Author contributions

Jianyi Yin, Chung-Ming Tse, and Mark Donowitz designed the experiments; Jianyi Yin, Chung-Ming Tse, Leela Rani Avula, Varsha Singh, and Jennifer Foulke-Abel performed experiments and analyzed data; Jianyi Yin drafted the manuscript; and Chung-Ming Tse, Hugo R. de Jonge, and Mark Donowitz revised the manuscript.

#### Conflicts of interest

The authors disclose no conflicts.

#### Funding

This study was supported in part by National Institutes of Health grants RO1 DK26523, RO1 DK61765, P01 DK072084, P30 DK089502, U01AI125181, UH3TR00003, U18TR000552, and R24 DK99803.